Personalized Federated Learning with Communication Compression

Anonymous authors
Paper under double-blind review

Abstract

In contrast to training traditional machine learning (ML) models in data centers, federated learning (FL) trains ML models over local datasets contained on resource-constrained heterogeneous edge devices. Existing FL algorithms aim to learn a single global model for all participating devices, which may not be helpful to all devices participating in the training due to the heterogeneity of the data across the devices. Recently, Hanzely and Richtárik (2020) proposed a new formulation for training personalized FL models aimed at balancing the trade-off between the traditional global model and the local models that could be trained by individual devices using their private data only. They derived a new algorithm, called *loopless gradient descent* (L2GD), to solve it and showed that this algorithms leads to improved communication complexity guarantees in regimes when more personalization is required. In this paper, we equip their L2GD algorithm with a *bidirectional* compression mechanism to further reduce the communication bottleneck between the local devices and the server. Unlike other compression-based algorithms used in the FL-setting, our compressed L2GD algorithm operates on a probabilistic communication protocol, where communication does not happen on a fixed schedule. Moreover, our compressed L2GD algorithm maintains a similar convergence rate as vanilla SGD without compression. To empirically validate the efficiency of our algorithm, we perform diverse numerical experiments on both convex and non-convex problems and using various compression techniques.

1 Introduction

We live in the era of big data, and mobile devices have become a part of our daily lives. While the training of ML models using the diverse data stored on these devices is becoming increasingly popular, the traditional data center-based approach to training them faces serious *privacy issues* and has to deal with *high communication and energy cost* associated with the transfer of data from users to the data center Dean et al. (2012). *Federated learning* (FL) provides an attractive alternative to the traditional approach as it aims to train the models directly on *resource constrained* heterogeneous devices without any need for the data to leave them Konečný et al. (2016); Kairouz et al. (2019).

The prevalent paradigm for training FL models is empirical risk minimization, where the aim is to train a *single global model* using the aggregate of all the training data stored across all participating devices. Among the popular algorithms for training FL models for this formulation belong FedAvg McMahan et al. (2017), Local GD Khaled et al. (2019; 2020), local SGD Stich (2019); Khaled et al. (2020); Gorbunov et al. (2020a) and Shifted Local SVRG Gorbunov et al. (2020a). All these methods require the participating devices to perform a local training procedure (e.g., by taking multiple steps of some optimization algorithm) and subsequently communicate the resulting model to an orchestrating server for aggregation; see Figure 1a. This process is repeated until a model of suitable qualities is found. For more variants of local methods and further pointers to the literature, we refer the reader to Gorbunov et al. (2020a).

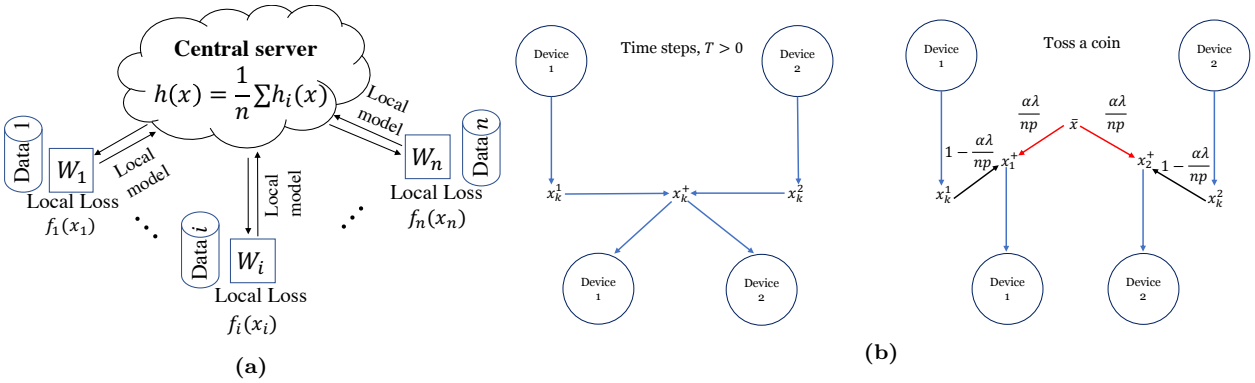

Figure 1: (a)Training n local devices, $\{W_i\}$ on the loss, f_i of their local model, x_i with a central server/master node, where h_i penalizes for dissimilarity between the local model, x_i and the average of all local models, $\bar{x}$. (b)FedAvg McMahan et al. (2017) and L2GD Hanzely & Richtárik (2020) algorithm on 2 devices. Unlike FedAvg, L2GD does not communicate after a fixed T local steps, it communicates based on a probabilistic protocol.

1.1 Personalized FL

In contrast, Hanzely & Richtárik (2020) recently introduced a new formulation of FL as an alternative to the existing "single-model-suits-all" approach embodied by empirical risk minimization. Their formulation explicitly aims to find a *personalized* model for every device; see Figure 1a. In particular, Hanzely & Richtárik (2020) considered the formulation[1]

$$\min_{x\in\mathbb{R}^{nd}} [F(x) := f(x) + h(x)] \tag{1}$$

for simultaneous training of n personalized FL models $x_1, \ldots, x_n \in \mathbb{R}^d$ for n participating devices. They chose

$$f(x) := \frac{1}{n}\sum_{i=1}^{n} f_i(x_i), \quad \text{and} \quad h(x) := \frac{1}{n}\sum_{i=1}^{n} h_i(x),$$

where f_i represents the loss of model x_i over the local data stored on device i. Function h_i penalizes for dissimilarity between the local model x_i and the average of all local models $\bar{x} := \frac{1}{n}\sum_{i=1}^{n} x_i$, and is defined to be

$$h_i(x) = \frac{\lambda}{2}\|x_i - \bar{x}\|_2^2,$$

where $\lambda > 0$ controls for the strength of this penalization. At one extreme, $\lambda \to \infty$ forces the local models to be equal to their average and hence mutually identical. Therefore, equation 1 reduces to the classical empirical risk minimization formulation of FL

$$\min_{z\in\mathbb{R}^d} \frac{1}{n}\sum_{i=1}^{n} f_i(z).$$

On the other hand, for $\lambda = 0$ problem equation 1 is equivalent to each client (node) training independently using their own data only. In particular, the i^{th} client solves

$$\min_{x_i\in\mathbb{R}^d} f_i(x_i).$$

By choosing λ to a value in between these two extremes, i.e., $0 < \lambda < \infty$, we control for the level of similarity we want the personalized models $\{x_i\}_{i=1}^n$ to posses.

We remark that, local methods such as FedAvg by McMahan et al. (2017) (also see similar methods in Haddadpour et al. (2019b); Stich (2019); Wang & Joshi (2019); Zhou & Cong (2018); Lin et al. (2019)), are popular for training FL models. Nevertheless, their main drawback in the heterogeneous setting with data and device heterogeneity is inefficient communication. Hanzely & Richtárik (2020) proposed this

[1]Zhang et al. (2015) considered a similar model in a different context and with different motivations.

new personalization to tackle heterogeneous data, and we are using their model to build our compressed, personalized FL.

To solve equation 1, Hanzely & Richtárik (2020) proposed a *probabilistic* gradient descent algorithm for which they coined the name loopless local gradient descent (L2GD). Hanzely & Richtárik (2020) shows how L2GD can be interpreted as a simple variant of FedAvg, typically presented as a method for solving the standard empirical risk minimization (ERM) formulation of FL. However, alongside Hanzely & Richtárik (2020) argue, L2GD is better seen as an algorithm for solving the personalized FL formulation equation 1. By doing so, they interpret the nature of local steps in classical FL: the role of local steps in classical FL methods is to provide personalization and not communication efficiency as was widely believed—FedAvg can diverge on highly non-identical data partitions McMahan et al. (2017). Instead, communication efficiency in local methods comes from their tendency to gear towards personalization, and personalized models are provably easier to train.

Communication compression. We observe that the *L2GD algorithm does not support any compression mechanism* for the master-worker and worker-master communication that needs to happen—This is the starting point of our work. *We believe that equipping personalized FL with fast and theoretically tractable communication compression mechanisms is an important open problem.* In distributed training of deep neural network (DNN) models, synchronous data-parallelism Dean et al. (2012) is most widely used and adopted by mainstream deep learning toolkits (such as `PyTorch, TensorFlow`). However, exchanging the stochastic gradients in the network for aggregation creates a communication bottleneck, and this results in slower training Xu et al. (2021a). One way to save on communication cost is to use compression operators Dan et al. (2017); Horváth et al. (2019); Xu et al. (2021a). Gradient compression techniques, such as quantization Dan et al. (2017); Bernstein et al. (2018); Horvath et al. (2019); Beznosikov et al. (2020); Safaryan et al. (2021), sparsification Suresh et al. (2017); Konečný & Richtárik (2018); Fikri & Kenneth (2017); Sahu et al. (2021); Stich et al. (2018); Dutta et al. (2020); Safaryan et al. (2021), hybrid compressors Strom (2015), and low-rank methods Vogels et al. (2019) have been proposed to overcome this issue. [2]

Although recent works have introduced compression in traditional FL formulation Konečný et al. (2016); Reisizadeh et al. (2020); Philippenko & Dieuleveut (2020); Shlezinger et al. (2020); Amiri et al. (2020); Xu et al. (2021b); except Horvath et al. (2019); Philippenko & Dieuleveut (2020); Gorbunov et al. (2020b); Amiri et al. (2020), others use compression only for the *throughput limited uplink* channel, that is, to upload the local models from the devices to the central server. But limited bandwidth in the downlink channel may pose a communication latency between the server and the devices and consequently, slow down the training; see detailed discussion in §2. As of now, no study combines *bidirectional* compression techniques with a probabilistic communication protocol in the FL set-up by using a mixture of a local and global model as in equation 1. In this work, we combine these aspects and make subsequent contributions.

1.2 Contributions

(i) **L2GD algorithm with bidirectional compression.** Communication compression is prevalent in recent local FL training algorithms, but these algorithms are not robust to data and device heterogeneity. L2GD by Hanzely & Richtárik (2020) remedies this issue by introducing personalization in FL. However, integrating compression with L2GD algorithm is a nontrivial task—unlike other FL algorithms, L2GD does not communicate after a fixed local steps, it communicates based on a probabilistic protocol; see §3 and Figure 1b. Additionally, due to this probabilistic protocol, the communication involves local model updates, as well as gradients; see §3. To reduce the communication bottleneck in L2GD, we use compression techniques on top of its probabilistic communication at both master and the participating local devices; see §4. To the best of our knowledge, we are the first to integrate *bidirectional compression techniques* with a probabilistic communication in the FL set-up, and we call our algorithm *compressed L2GD*; see Algorithm 1.

(ii) **Convergence analysis.** In §5, we prove the convergence of our *compressed L2GD* algorithm based on the most recent theoretical development, such as expected smoothness as in Gower et al. (2019). Admittedly, convergence analysis of first-order optimization algorithms with bidirectional compression exists in the

[2]Model compression Guo (2018); Chraibi et al. (2019) is orthogonal to gradient compression and not in the scope of this work.

literature, see Tang et al. (2019); Horvath et al. (2019); Amiri et al. (2020); Dutta et al. (2020), integrating arbitrary unbiased compressors with a probabilistic communication protocol into personalized FL, and showing convergence are nontrivial and the first one in its class. Our compressed L2GD algorithm maintains a similar asymptotic convergence rate as the baseline vanilla SGD without compression in both strongly convex and smooth nonconvex cases; see Theorem 1 and 2 in §5.

(*iii*) **Optimal rate and communication.** We optimized the complexity bounds of our algorithm as a function of the parameters involved in the algorithm. This leads us to the "optimal" setting of our algorithm. Mainly, we derived the optimal expected number of local steps to get the optimal iteration complexity and communication rounds; see §6. Although our analysis is based on some hard-to-compute constants in real life, e.g., Lipchitz constant, this may help the practitioners to get an insight into the iteration complexity and communication trade-off; see Theorem 3 and 4 in §6.

(*iv*) **Empirical study.** We perform diverse numerical experiments on synthetic and real datasets by using both convex and non-convex problems (using 4 DNN models) and invoking various compression techniques; see details in §7, Table 1. In training larger DNN models, to obtain the same global Top-1 test accuracy, compressed L2GD reduces the communicated data-volume (bits normalized by the number of local devices or clients, #bits/n), from 10^{15} to 10^{11}, rendering approximately 10^4 times improvement compared to FedAvg; see §7.2. Moreover, L2GD with natural compressor (that by design has smaller variance) empirically behaves the best and converges approximately 5 times faster, and reaches the best accuracy on both train and the test sets compared to no-compression FedOpt Reddi et al. (2020) baseline; see §7.2 and §A.2. These experiments validate the effect of the parameters used, effect of compressors, and show the efficiency of our algorithm in practice.

2 Related Work

Numerous studies are proposed to reduce communication but not all of them are in the FL setting. In this scope, for completeness, we quote a few representatives from each class of communication efficient SGD.

Smith et al. in Smith et al. (2017) proposed a communication-efficient primal-dual optimization that learns separate but related models for each participating device. FedAvg by McMahan et al. (2017) performs local steps on a subset of participating devices in an FL setting. Similar to FedAvg, but without data and device heterogeneity, Haddadpour et al. (2019b); Stich (2019); Wang & Joshi (2019); Zhou & Cong (2018); Lin et al. (2019) independently proposed local SGD, where several local steps are taken on the participating devices before periodic communication and averaging the local models. While FedProx by Li et al. (2020) is a generalization of FedAvg, SCAFFOLD uses a variance reduction to correct local updates occurring from an non-i.i.d data in FedAvg. From the system's perspective, on `TensorFlow`, Bonawitz et al. (2019) built a FL system on mobile devices.

Compression has also been introduced in the FL setup. Shlezinger et al. Shlezinger et al. (2020) combined universal vector quantization with FL for throughput limited uplink channel. In FedPAQ by Reisizadeh et al. Reisizadeh et al. (2020), each local device sends a compressed difference between its input and output model to the central server, after computing the local updates for a fixed number of iterations. While Amiri et al. (2020) used a bidirectional compression in FL set-up, Philippenko & Dieuleveut (2020) combined it with a memory mechanism or error feedback Stich et al. (2018).

Among other proposed communication efficient SGDs, parallel restarted SGD Yu et al. (2019a) reduces the number of communication rounds compare to the baseline SGD. Farzin et al. Haddadpour et al. (2019a) showed that redundancy reduces residual error as compared with the baseline SGD where all nodes can sample from the complete data and this leads to lower communication overheads. CoCoA by Jaggi et al. (2014), Dane by Shamir et al. Shamir et al. (2014) perform several local steps and hence fewer communication rounds before communicating with the other workers. Lazily aggregated gradient (LAG) algorithm by Chen et al. (2018a) selects a subgroup of workers and uses their gradients, instead of obtaining a fresh gradient from each worker in each iteration.

In decentralized training, where the nodes only communicate with their neighbors, Koloskova et al. (2019) implemented an *average consensus* where the nodes can communicate to their neighbors via a fixed

communication graph. Li et al. (2018) proposed Pipe-SGD—a framework with decentralized pipelined training and balanced communication.

Personalization in FL is a growing research area. Arivazhagan et al. Arivazhagan et al. (2019) proposed FedPer to mitigate statistical heterogeneity of data; also see adaptive personalized FL algorithm in Deng et al. (2020). Mei et al. Mei et al. (2021) proposed to obtain personalization in FL by using layer-wise parameters, and two-stage training; also see Ma et al. (2022) and model personalization in Shen et al. (2022). Shamsian et al. Shamsian et al. (2021) trained a central hypernetwork model to generate a set of personalized models for the local devices. Li et al. Li et al. (2021) proposed Hermes—a communication-efficient personalized FL, where each local device identifies a small subnetwork by applying the structured pruning, communicates these subnetworks to the server and the devices, the server performs the aggregation on only overlapped parameters across each subnetwork; also see Pillutla et al. (2022) for partial model personalization in FL. DispFL is another communication-efficient personalized FL algorithm proposed by Dai et al. Dai et al. (2022). In recent work, Zhang et al. Zhang et al. (2021) introduce personalization by calculating optimal weighted model combinations for each client without assuming any data distribution. For connection between personalization in FL and model-agnostic-meta-learning (MAML), see Fallah et al. (2020). Additionally, we refer to the surveys Kulkarni et al. (2020); Tan et al. (2022) for an overview of personalization in FL.

3 Background and Preliminaries

Notation. For a given vector, $x \in \mathbb{R}^{nd}$, by x_i we denote the i^{th} subvector of x, and write $x = \left(x_1^\top, \ldots, x_n^\top\right)^\top$, where $x_i \in \mathbb{R}^d$. We denote the i^{th} component of x by $x_{(i)}$ and $\|x\|$ represents its Euclidean norm. By $[n]$ we denote the set of indexes, $\{1, \ldots, n\}$. By $\mathbb{E}_\xi(\cdot)$ we define the expectation over the randomness of ξ conditional to all the other potential random variables. The operator, $\mathcal{C}(\cdot) := \left(\mathcal{C}_1(\cdot)^\top, \ldots, \mathcal{C}_n(\cdot)^\top\right)^\top : \mathbb{R}^{nd} \to \mathbb{R}^{nd}$ denotes a compression operator with each $\mathcal{C}_i(\cdot)$ being compatible with x_i. Denote $Q := [I, I, \ldots, I]^\top \in \mathbb{R}^{nd \times d}$, where I denotes the identity matrix of $\mathbb{R}^{d \times d}$. With our Assumptions that we will introduce later in the paper, the problem equation 1 has a unique solution, which we denote by x^* and we define $\bar{x}^*$ as $\bar{x}^* = \frac{1}{n}\sum_{i=1}^n x_i^*$. By $|S|$ we denote the cardinality of a set, S.

Loopless local gradient descent (L2GD). We give a brief overview of the loopless local gradient descent (L2GD) algorithm by Hanzely & Richtárik (2020) to solve equation 1 as a two sum problem. At each iteration, to estimate the gradient of F, L2GD samples either the gradient of f or the gradient of h and updates the local models via:

$$x_i^{k+1} = x_i^k - \alpha G_i(x^k), \ i = 1, \ldots, n,$$

where $G_i(x^k)$ for $i = 1, \ldots, n$, is the i^{th} block of the vector

$$G(x^k) = \begin{cases} \frac{\nabla f(x^k)}{1-p} & \text{with probability } 1-p, \\ & \textbf{(Local gradient step)} \\ \frac{\nabla h(x^k)}{p} & \text{with probability } p, \\ & \textbf{(Aggregation step)} \end{cases}$$

where $0 < p < 1$, $\nabla f(x^k)$ is the gradient of f at x^k, and $\nabla_i h(x^k) = \frac{\lambda}{n}\left(x_i^k - \bar{x}^k\right)$ is the i^{th} block of the gradient of h at x^k.

In this approach, there is a hidden communication between the local devices because in aggregation steps they need the average of the local models. That is, the communication occurs when the devices switch from a local gradient step to an aggregation step. Note that there is no need for communication between the local devices when they switch from an aggregation step to a local gradient step. There is also no need for communication after two consecutive aggregation steps since the average of the local models does not change in this case. If k and $k+1$ are both aggregation steps, we have $\bar{x}^{k+1} = \frac{1}{n}\sum_{i=1}^n x_i^{k+1} = \frac{1}{n}\sum_{i=1}^n x_i^k - \frac{\alpha\lambda}{n}\frac{1}{n}\sum_{i=1}^n \left(x_i^k - \bar{x}^k\right) = \bar{x}^k$.

4 Compressed L2GD

Now, we are all set to describe the compressed L2GD algorithm for solving (1). We start by defining how the compression operates in our set-up.

4.1 Compressed communication

Recall that original L2GD algorithm has a probabilistic communication protocol—the devices do not communicate after every fixed number of local steps. The communication occurs when the devices switch from a local gradient step to an aggregation step. Therefore, instead of using the compressors in a fixed time stamp (after every $T > 0$ iterations, say), each device i, requires to compress its local model x_i when it needs to communicate it to the master, based on the probabilistic protocol. We assume that device i uses the compression operator, $\mathcal{C}_i(\cdot) : \mathbb{R}^d \to \mathbb{R}^d$. Moreover, another compression happens when the master needs to communicate with the devices. We assume that the master uses the compression operator, $\mathcal{C}_M(\cdot) : \mathbb{R}^d \to \mathbb{R}^d$. Therefore, the compression is used in uplink and downlink channels similar to Dutta et al. (2020); Horvath et al. (2019), but occurs in a probabilistic fashion. There exists another subtlety—although the model parameters (either from the local devices or the global aggregated model) are communicated in the network for training FL model via compressed L2GD, the compressors that we use in this work are the compressors used for gradient compression in distributed DNN training; see Xu et al. (2021a).

4.2 The Algorithm

Note that, in each iteration $k \geq 0$, there exists a random variable, $\xi_k \in \{0, 1\}$ with $P(\xi_k = 1) = p$ and $P(\xi_k = 0) = 1 - p$. If $\xi_k = 0$, all local devices at iteration k, perform one local gradient step. Otherwise (if $\xi_k = 1$), all local devices perform an aggregation step. However, to perform an aggregation step, the local devices need to know the average of the local models. If the previous iteration (i.e, $k - 1^{\text{th}}$ iteration) was an aggregation step (i.e, $\xi_{k-1} = 1$), then at the current iteration the local devices can use the same average as the one at iteration $k - 1$ (recall, the average of the local models does not change after two consecutive aggregation steps). Otherwise a communication happens with the master to compute the average. In this case, each local device i compresses its local model x_i^k to $\mathcal{C}_i(x_i^k)$ and communicates the result to the master. The master computes the average based on the compressed values of local models:

$$\bar{y}^k := \frac{1}{n} \sum_{j=1}^{n} \mathcal{C}_j(x_j^k),$$

then it compresses $\bar{y}^k$ to $\mathcal{C}_M(\bar{y}^k)$ by using compression operator at the master's end and communicates it back to the local devices. The local devices further perform an aggregation step by using $\mathcal{C}_M(\bar{y}^k)$ instead of the exact average. This process continues until convergence. From Algorithm 1, we have, for $i = 1, \ldots, n$:

$$x_i^{k+1} = x_i^k - \eta G_i(x^k),$$

where

$$G_i(x^k) = \begin{cases} \frac{\nabla f_i\left(x_i^k\right)}{n(1-p)} & \text{if } \xi_k = 0 \\ \frac{\lambda}{np}\left(x_i^k - \mathcal{C}_M(\bar{y}^k)\right) & \text{if } \xi_k = 1 \ \& \ \xi_{k-1} = 0, \\ \frac{\lambda}{np}\left(x_i^k - \bar{x}^k\right) & \text{if } \xi_k = 1 \ \& \ \xi_{k-1} = 1. \end{cases}$$

We give the pseudo code in Algorithm 1.

5 Convergence Analysis

With the above setup, we now prove the convergence of Algorithm 1; see detailed proofs in §A.1.

5.1 Assumptions

We make the following general assumptions in this paper.

Algorithm 1 Compressed L2GD

Input: $\{x_i^0\}_{i=1,\dots,n}$, stepsize $\eta > 0$, probability p, $\xi_{-1} = 1$, $\bar{x}^{-1} = \frac{1}{n}\sum_{i=1}^n x_i^0$.
for $k = 0, 1, 2, \dots$ **do**
  Draw: $\xi_k = 1$ with probability p
  if $\xi_k = 0$ **then**
    on all devices: $x_i^{k+1} = x_i^k - \frac{\eta}{n(1-p)}\nabla f_i(x_i^k)$ for $i \in [n]$
  else
    if $\xi_{k-1} = 0$ **then**
      on all devices: Compress x_i^k to $\mathcal{C}_i(x_i^k)$ and communicate $\mathcal{C}_i(x_i^k)$ to the master
      on master: receive $\mathcal{C}_i(x_i^k)$ from the device i, for all $i \in [n]$ compute $\bar{y}^k := \frac{1}{n}\sum_{j=1}^n \mathcal{C}_j(x_j^k)$ compress $\bar{y}^k$ to $\mathcal{C}_M(\bar{y}^k)$ and communicate it to all devices
      on all devices: Perform aggregation step $x_i^{k+1} = x_i^k - \frac{\eta\lambda}{np}\left(x_i^k - \mathcal{C}_M(\bar{y}^k)\right)$
    else
      on all devices: $\bar{x}^k = \bar{x}^{k-1}$, Perform aggregation step $x_i^{k+1} = x_i^k - \frac{\eta\lambda}{np}\left(x_i^k - \bar{x}^k\right)$
    end if
  end if
end for

Assumption 1 *For $i = 1, \dots, n$:*

- *The compression operator, $\mathcal{C}_i(\cdot) : \mathbb{R}^d \to \mathbb{R}^d$ is unbiased,*

$$\mathbb{E}_{\mathcal{C}_i}\left[\mathcal{C}_i(x)\right] = x, \quad \forall x \in \mathbb{R}^d.$$

- *There exists constant, $\omega_i > 0$ such that the variance of $\mathcal{C}_i$ is bounded as follows:*

$$\mathbb{E}_{\mathcal{C}_i}\left[\|\mathcal{C}_i(x) - x\|^2\right] \leq \omega_i\|x\|^2, \forall x \in \mathbb{R}^d.$$

- *The operators, $\{\mathcal{C}_i(\cdot)\}_{i=1}^n$ are independent from each other, and independent from ξ_k, for all $k \geq 0$.*
- *The compression operator, $\mathcal{C}_M(\cdot)$ is unbiased, independent from $\{\mathcal{C}_i\}_{i=1}^n$ and has compression factor, ω_M.*

From the above assumption we conclude that for all $x \in \mathbb{R}^d$, we have

$$\mathbb{E}_{\mathcal{C}_i}\left[\|\mathcal{C}_i(x)\|^2\right] \leq (1 + \omega_i)\|x\|^2.$$

The following lemma characterizes the compression factor, ω of the joint compression operator, $\mathcal{C}(\cdot) = \left(\mathcal{C}_1(\cdot)^\top, \dots, \mathcal{C}_n(\cdot)^\top\right)^\top$ as a function of $\omega_1, \dots, \omega_n$.

Lemma 1 *Let $x \in R^{nd}$, then*

$$\mathbb{E}_{\mathcal{C}}\left[\|\mathcal{C}(x)\|^2\right] \leq (1 + \omega)\|x\|^2,$$

where $\omega = \max_{i=1,\dots,n}\{\omega_i\}$.

Our next assumption is on the function f.

Assumption 2 *We assume that f is L_f-smooth and μ-strongly convex.*

5.2 Auxiliary results

Before we state our main convergence theorem, we state several intermediate results needed for the convergence. In the following two lemmas, we show that based on the randomness of the compression operators, in expectation, we recover the exact average of the local models and the exact gradients for all iterations.

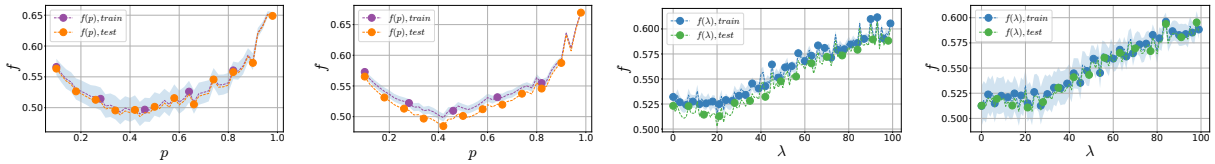

(a) **(b)** **(c)** **(d)**

Figure 2: Uncompressed L2GD on $n = 5$ workers. We show the loss, f as a function of p and λ obtained after $K = 100$ iterations of Algorithm 1 with $\mathcal{C}$ an identity compressor. (a) `a1a` dataset, $d = 124, \lambda = 10$, (b) `a2a` dataset, $d = 124, \lambda = 10$, (c) `a1a` dataset, $d = 124, p = 0.65$ (d) `a2a` dataset, $d = 124, p = 0.65$.

Lemma 2 *Let Assumption 1 hold, then for all $k \geq 0$, $\mathbb{E}_{\mathcal{C},\mathcal{C}_M}\left[\mathcal{C}_M(\bar{y}^k)\right] = \bar{x}^k$.*

Lemma 3 *Let Assumptions 1 hold. Then for all $k \geq 0$, knowing x^k, $G(x^k)$ is an unbiased estimator of the gradient of function F at x^k.*

Our next lemma gives an upper bound on the iterate at each iteration. This bound is composed of two terms—the optimality gap, $F(x^k) - F(x^*)$, and the norm at the optimal point, x^*.

Lemma 4 *Let Assumption 2 hold, then*

$$\left\|x^k\right\|^2 \leq \frac{4}{\mu}\left(F(x^k) - F(x^*)\right) + 2\left\|x^*\right\|^2.$$

Lemma 5 helps us to prove the expected smoothness property Gower et al. (2019). The bound in Lemma 5 is composed of—the optimality gap, the difference between the gradients of h at x^k and x^*, and an extra constant, β that depends on the used compressors.

Lemma 5 *Let Assumptions 1 and 2 hold. Then*

$$\begin{aligned}\mathcal{A} &:= \mathbb{E}_{\mathcal{C}_M,\mathcal{C}}\left\|x^k - Q\mathcal{C}_M(\bar{y}^k) - x^* + Q\mathcal{C}_M(\bar{y}^*)\right\|^2 \\ &\leq \tfrac{4n^2}{\lambda^2}\left\|\nabla h(x^k) - \nabla h(x^*)\right\|^2 + \alpha\left(F(x^k) - F(x^*)\right) + \beta,\end{aligned}$$

where $\bar{y}^* := \frac{1}{n}\sum_{j=1}^n \mathcal{C}_j(x_j^*)$, $\alpha := \frac{4(4\omega+4\omega_M(1+\omega))}{\mu}$, and

$$\beta \quad := \quad 2\left(4\omega + 4\omega_M(1+\omega)\right)\left\|x^*\right\|^2 + 4\mathbb{E}_{\mathcal{C}_M,\mathcal{C}}\left\|Q\mathcal{C}_M(\bar{y}^*) - Q\bar{x}^*\right\|^2.$$

Lemma 6 is the final result that (together with Lemma 5) shows the expected smoothness property and gives an upper bound on the stochastic gradient. This bound is composed of three terms—the optimality gap, $F(x^k) - F(x^*)$, the expected norm of the stochastic gradient at the optimal point, $\mathbb{E}\|G(x^*)\|^2$, and some other quantity that involves interplay between the parameters used in Algorithm 1 and the used compressor.

Lemma 6 (Expected Smoothness) *Let Assumptions 1 and 2 hold, then*

$$\mathbb{E}\left[\|G(x^k)\|^2 | x^k\right] \leq 4\gamma\left(F(x^k) - F(x^*)\right) + \delta, \tag{2}$$

where

$$\gamma := \tfrac{\alpha\lambda^2(1-p)}{2n^2p} + \max\left\{\tfrac{L_f}{(1-p)}, \tfrac{\lambda}{n}\left(1 + \tfrac{4(1-p)}{p}\right)\right\}$$

and

$$\delta := \frac{2\beta\lambda^2(1-p)}{n^2p} + 2\mathbb{E}\|G(x^*)\|^2.$$

Remark 1 *If there is no compression, the operators, $\mathcal{C}_i(\cdot)$, for $i \in [n]$, and $\mathcal{C}_M(\cdot)$ are equal to identity. The compression constants, ω_i, for $i \in [n]$, and ω_M are equal to zero. Therefore, $\alpha = \beta = 0$, and the factor 4 in the formula of γ can be replaced by 1 and thus*

$$\delta = \tfrac{2\beta\lambda^2(1-p)}{n^2 p} + 2\mathbb{E}\|G(x^*)\|^2 = 2\mathbb{E}\|G(x^*)\|^2,$$

with

$$\gamma = \max\left\{\tfrac{L_f}{(1-p)}, \tfrac{\lambda}{n}\left(1 + \tfrac{(1-p)}{p}\right)\right\} = \max\left\{\tfrac{L}{n(1-p)}, \tfrac{\lambda}{np}\right\},$$

where $L = nL_f$. Same constants arise in the expected smoothness property in Hanzely & Richtárik (2020).

5.3 Main result

We now state the convergence result for Algorithm 1 for both strongly convex and nonconvex cases.

Theorem 1 *(Strongly convex case) Let Assumptions 1 and 2 hold. If $\eta \leq \frac{1}{2\gamma}$, then*

$$\mathbb{E}\left\|x^k - x^*\right\|^2 \leq \left(1 - \tfrac{\eta\mu}{n}\right)^k \left\|x^0 - x^*\right\|^2 + \tfrac{n\eta\delta}{\mu}.$$

Proof 1 *The proof follows directly from Lemma 3, 6, and Theorem 3.1 from Gower et al. (2019).*

Theorem 2 *(Non convex case) Let Assumption 1 hold. Assume also that F is L-smooth, bounded from below by $F(x^*)$. Then to reach a precision, $\epsilon > 0$, set the stepsize, $\eta = \min\{\frac{1}{\sqrt{2L\gamma K}}, \frac{\epsilon^2}{L\delta}\}$, such that for $K \geq \frac{6L}{\epsilon^4}\max\{12\gamma(F(x^0) - F(x^*))^2, \delta\}$, we have $\min_{k=0,1,\ldots,K}\mathbb{E}\|\nabla F(x^k)\|_2 \leq \epsilon$.*

Remark 2 *For smooth non-convex problems, we recover the optimal $O(\epsilon^4)$ classical rate as vanilla SGD.*

6 Optimal Rate and Communication

In this section, we provide the "optimal" setting of our algorithm that is obtained by optimizing the complexity bounds of our algorithm as a function of the parameters involved. The analysis on this section is based on the following upper bound of γ. We recall that

$$\begin{aligned}\gamma &= \frac{\alpha\lambda^2(1-p)}{2n^2p} + \max\left\{\frac{L_f}{(1-p)}, \frac{\lambda}{n}\left(1 + \frac{4(1-p)}{p}\right)\right\} \\ &\leq \frac{\alpha\lambda^2(1-p)}{2n^2p} + \max\left\{\frac{L_f}{(1-p)}, \frac{4\lambda}{np}\right\} := \gamma_u.\end{aligned}$$

Note that the number of iterations is linearly dependent on γ. Therefore, to minimize the total number of iterations, it suffices to minimize γ. Define $L := nL_f$.

Theorem 3 (Optimal rate) *The probability p^* minimizing γ is equal to $\max\{p_e, p_A\}$, where $p_e = \frac{7\lambda + L - \sqrt{\lambda^2 + 14\lambda L + L^2}}{6\lambda}$ and p_A is the optimizer of the function $A(p) = \frac{\alpha\lambda^2}{2n^2p} + \frac{L}{n(1-p)}$ in $(0,1)$.*

Remark 3 *If we maximize the upper bound, γ_u instead of γ then p_e simplifies to $\frac{4\lambda}{L+4\lambda}$.*

Lemma 7 *The optimizer probability p_A of the function $A(p) = \frac{\alpha\lambda^2}{2n^2p} + \frac{L}{n(1-p)}$ in $(0,1)$ is equal to*

$$p_A = \begin{cases} \frac{1}{2} & \text{if } 2nL = \alpha\lambda^2 \\ \frac{-2\alpha\lambda^2 + 2\lambda\sqrt{2\alpha nL}}{2(2nL - \alpha\lambda^2)} & \text{if } 2nL > \alpha\lambda^2 \\ \frac{-2\alpha\lambda^2 - 2\lambda\sqrt{2\alpha nL}}{2(2nL - \alpha\lambda^2)} & \text{otherwise.} \end{cases}$$

Table 1: Gradient compression methods used in this work. Note that $\|\tilde{g}\|_0$ and $\|g\|_0$ are the number of elements in the compressed and uncompressed gradient, respectively; nature of operator Q is random or deterministic. We implement that mechanisms for FedML.ai framework.

Compression	Ref.	Similar Methods	$\|\tilde{g}\|_0$	Nature of $\mathcal{C}$
QSGD	Dan et al. (2017)	Horvath et al. (2019); Wang et al. (2018); Wen et al. (2017) Wu et al. (2018); Yu et al. (2019b); Zhang et al. (2017)	$\|g\|_0$	Rand, unbiased
Natural	Horvath et al. (2019)	Dan et al. (2017); Yu et al. (2019b); Zhang et al. (2017)	$\|g\|_0$	Rand, unbiased
TernGrad	Wen et al. (2017)	Dan et al. (2017); Wang et al. (2018); Yu et al. (2019b)	$\|g\|_0$	Rand, unbiased
Bernoulli	Khirirat et al. (2018)	—	—	Rand, unbiased
Top-k	Fikri & Kenneth (2017)	Alistarh et al. (2018); Stich et al. (2018)	k	Det, Biased

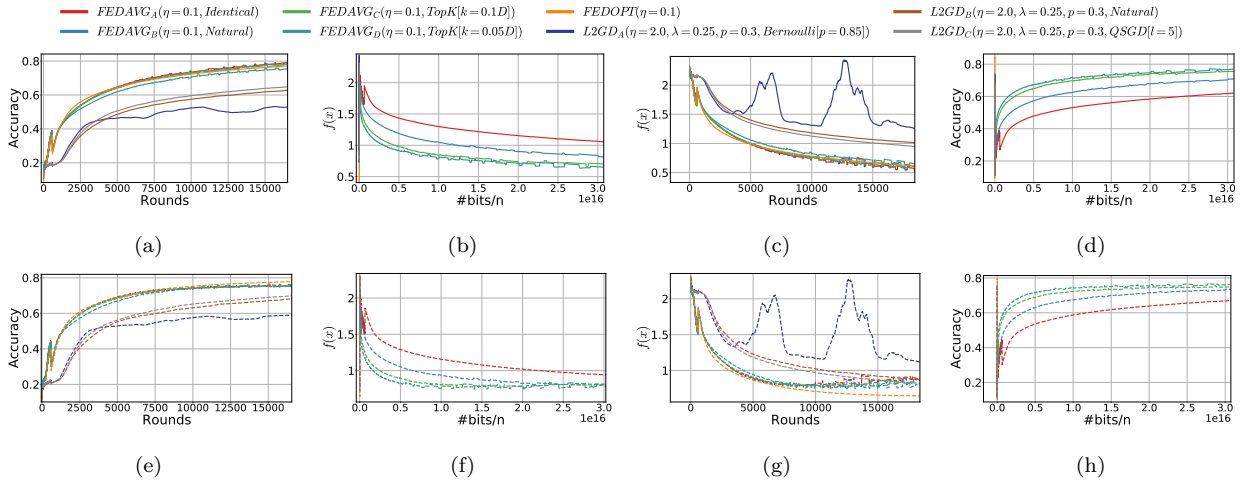

Figure 3: Training `ResNet-18` on `CIFAR-10` with $n = 10$ workers. The top row represents the Top-1 accuracy vs. rounds in (a), loss functional value vs. communicated bits in (b), loss functional value vs. rounds in (c), and Top-1 accuracy vs. communicated bits in (d) on the train set. The bottom row presents the similar plots on the Test set in (e)–(h).

Note that the number of communication rounds is linearly proportional to $C := p(1-p)\gamma$. Therefore, minimizing the total number of communication rounds suffices to minimize C or nC.

Theorem 4 (Optimal communication) *The probability p^* optimizing C is equal to* $\max\{p_e, p_A\}$*, where* $p_e = \frac{7\lambda+L-\sqrt{\lambda^2+14\lambda L+L^2}}{6\lambda}$ *and* $p_A = 1 - \frac{Ln}{\alpha\lambda^2}$.

Remark 4 *As in Remark 3, we note that, if we use the upper bound, γ_u instead of γ then p_e simplifies to* $\frac{4\lambda}{L+4\lambda}$.

We note that $\lambda \to 0$ implies $p^* \to 0$. This means that the optimal strategy, in this case, is *no communication at all*. This result is intuitive since for $\lambda = 0$, we deal with pure local models which can be computed without any communication. As $\lambda \to \infty$ implies $p^* \to 1$ denoting that the optimal strategy is to communicate often to find the global model.

7 Empirical study

We conducted diverse numerical experiments with L2GD algorithm that includes: (*i*) Analysis of algorithm meta-parameters for logistic regression in strongly convex setting; see §7.1; (*ii*) analysis of compressed L2GD algorithm on image classification with DNNs; see §7.2.

Computing environment. We performed experiments on server-grade machines running Ubuntu 18.04 and Linux Kernel v5.4.0, equipped with 8-cores 3.3 GHz Intel Xeon and a single NVIDIA GeForce RTX 2080

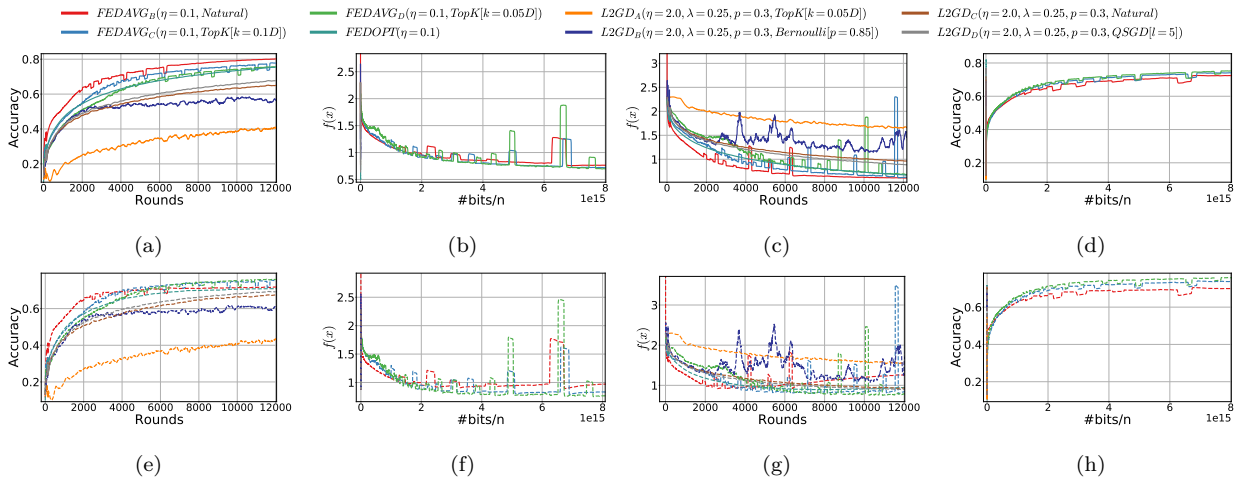

Figure 4: Training `DenseNet-121` on `CIFAR-10` with $n = 10$ workers. The top row represents the Top-1 accuracy vs. rounds in (a), loss functional value vs. communicated bits in (b), loss functional value vs. rounds in (c), and Top-1 accuracy vs. communicated bits in (d) on the train set. The bottom row presents the similar quantities on the Test set in (e)–(h).

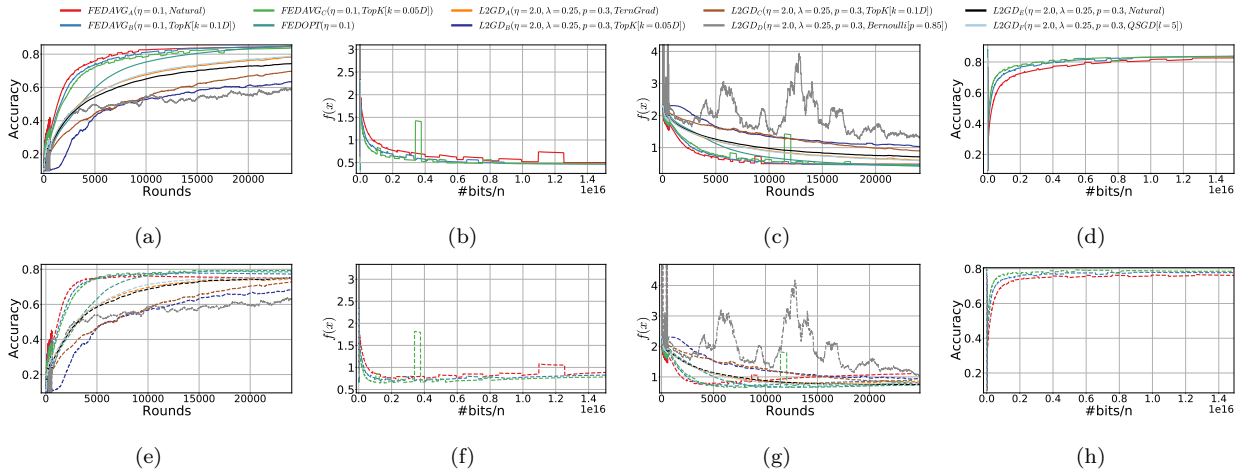

Figure 5: Training `MobileNet` on `CIFAR-10` with $n = 10$ workers. The top row represents the Top-1 accuracy vs. rounds in (a), loss functional value vs. communicated bits in (b), loss functional value vs. rounds in (c), and Top-1 accuracy vs. communicated bits in (d) on the train set. The bottom row presents the similar plots on the Test set in (e)–(h).

Ti.Tesla-V100-SXM2 GPU with 32GB of GPU memory. The computation backend for Logistics Regression experiments was NumPy library with leveraging MPI4PY for inter-node communication. For DNNs we used recent version of FedML He et al. (2020) benchmark[3] and patched it with: (*i*) distributed and standalone version of Algorithm 1; (*ii*) serializing and plotting mechanism; (*iii*) modifications in standalone, distributed version of FedAvg McMahan et al. (2017) and FedOpt Reddi et al. (2020) to be consistent with equation 1; (*iv*) not to drop the last batch while processing the dataset.

7.1 Meta-parameter study

The purpose of these experiments is to study the meta-parameters involved in uncompressed L2GD algorithm. We used L2GD algorithm without compression for solving ℓ_2 regularized logistic regression on LIBSVM `a1a` and `a2a` datasets Chang & Lin (2011). Both datasets contain shuffled examples in the train set, and we did

[3]FedML.AI

Model	Training parameters	L2GD bits/n	Baseline bits/n
DenseNet-121	79×10^5	8×10^{11}	$4 \cdot 10^{15}$
MobileNet	32×10^5	1.7×10^{11}	1×10^{15}
ResNet-18	11×10^6	1.1×10^{12}	1.5×10^{16}

Table 2: Summary of the benchmarks. The measured quantity is bits/n to achieve 0.7 Top-1 test accuracy, with $n = 10$ clients. For DenseNet-121, MobileNet, Resnet-18 the baseline is FedAvg with natural compressor with 1 local epoch; L2GD also uses natural compressor.

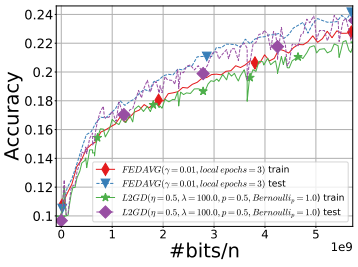

Figure 6: FedAvg as a particular case of L2GD: Test and train accuracy for ResNet-56 on CIFAR-10.

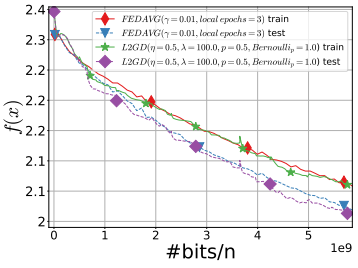

Figure 7: FedAvg as a particular case of L2GD: Test and train loss for ResNet-56 on CIFAR-10.

not perform any extra shuffling. To simulate the FL settings, we divided both datasets into 5 parts. After splitting, each worker has 321 and 453 records for `a1a`, and `a2a`, respectively.

Setup and results. We define $f_i(x)$ to be local empirical risk minimization for logistic loss with additive regularization term for local data D_i and of the form:

$$f_i(x) = \frac{1}{n_i} \sum_{j=1}^{n_i} \log(1 + \exp(-b^{(j)} x^\top a^{(j)})) + \frac{L_2}{2} \|x\|^2,$$

where $a^{(j)} \in \mathbb{R}^{124}, b^{(j)} \in \{+1, -1\}, n_i = |D_i|$. We set $L_2 = 0.01$, and varied meta-parameters p and λ. For each parameter, we performed 100 iterations of Algorithm 1. Note that, as meta-parameter λ decreases the models will fit more to its local data, while p provides stochastic balance between local gradient steps with probability, $1 - p$ and aggregation with probability, p.

Takeaway message. The results in Figure 2 support the theoretical finding—there exists an optimal choice of (p, λ), where the loss function, f achieves the least value. Nevertheless, this choice is problem dependent. Additionally, we find small p is not good due to lack of samples in a single node compared to samples available at other nodes. There is a trade-off for each node in learning from the other nodes' data and spending time to learn from its own data. In the experiments, the "optimal" setting of our algorithm is attained for $p = 0.4$ and λ in $[0, 25]$. Finally, we observe that *to get the smallest errors on the training and validation sets, it is better not to perform the averaging step too often.*

7.2 Training DNN models

We choose three practically important DNN models used for image classification, and other down-streaming tasks, such as feature extractions for image segmentation, object detection, image embedding, image captioning, to name a few.

- `ResNet-18` He et al. (2016). The overwhelmingly popular `ResNet` architecture exploits residual connections to remedy vanishing gradients. The network supported the trend toward smaller filters and deeper architectures, more curated towards FL training. Additionally, we use `ResNet-56` He et al. (2016).
- `DenseNet` Huang et al. (2017) contains a short connection between layers via connecting each layer to every other layer in a feed-forward fashion. Dense connection allows propagating information to the final classifier via concatenating all feature maps. Each layer in `DenseNet` is narrow and contains only 12 filters—another practical model for FL training.
- `MobileNet` Howard et al. (2017). DNN architecture has a trade off between computational complexity and accuracy (Bianco et al., 2018, p.3, Fig.1). For mobile devices that appear in cross-device FL, the

computation cost and energy consumption are both important. The energy consumption is mostly driven by memory movement Chen et al. (2018b), Horowitz (2014). In `MobileNet` architecture standard convolution blocks performs depth-wise convolution followed by 1×1 convolution. This is computationally less expensive in flops during inference time (see (Bianco et al., 2018, Fig.1, p.3)) and is $\sim 3.5\times$ more power efficient compare to `DenseNet` (García-Martín et al., 2019, p.85, Table 7). This makes `MobileNet` an attractive model for FL training.

Dataset and Setup. We consider `CIFAR-10` dataset Krizhevsky & Hinton (2009) for image classification. It contains color images of resolution 28×28 from 10 classes. The training and the test set are of size, 5×10^4 and 10^4, respectively. The training set is partitioned heterogeneously across 10 clients. The proportion of samples of each class stored at each local node is drawn by using the Dirichlet distribution ($\alpha = 0.5$). In our experiments, all clients are involved in each communication round. Additionally, we added a linear head in all CNN models for `CIFAR-10`, as they are originally designed for classification task with 1000 output classes.

Loss function. Denote $f_i(x) = w_i \cdot \frac{1}{|D_i|} \sum_{(a_i,b_i)\in D_i} l(a_i, b_i, x)$ to be a weighted local empirical risk associated with the local data, $\mathcal{D}_i$ stored in node, i. We note that $l(a_i, b_i, x)$ is a standard unweighted cross-entropy loss, $a_i \in \mathbb{R}^{28\times 28\times 3}$, $b_i \in \{0, 1\}^{10}$ with only one component equal to 1, the ground truth value, and the weight is set to $w_i = |D_i|/|D_1 \cup \cdots \cup D_n|$.

Metrics. To measure the performance, we examine the loss function value, $f(x)$, and the Top-1 accuracy of the global model on both train and the test set. Additionally, we measure the number of rounds, and bits/n—communicated bits normalized by the number of local clients, n. The intuition behind using the last metric is to measure the commmunicated data-volume; it is widely *hypothesized* that the reduced data-volume translates to a faster training in a constant speed network in distributed setup Gajjala et al. (2020); Xu et al. (2021a).

Compressors used. The theoretical results of compressed L2GD are attributed to unbiased compressors. We used 4 different unbiased compressors at the clients: Bernoulli Khirirat et al. (2018), natural compressor Horvath et al. (2019), random dithering a.k.a. QSGD Dan et al. (2017), and Terngrad Wen et al. (2017); see Table 1 for details. Additionally, we note that biased compressors (mostly sparsifiers) are popular in DNN training. Therefore, out of scientific curiosity, we used a popular sparsifier: Top-k Fikri & Kenneth (2017); Sahu et al. (2021) as a proof of concept. We note that extending the compressed L2GD theory for biased compressors (with or without error-feedback Xu et al. (2021a)) is nontrivial and mathematically involved, and left for future work.

Algorithms used for comparison. We used state-of-the-art FL training algorithms, FedAvg McMahan et al. (2017) and FedOpt Reddi et al. (2020) as no compression baseline to compare against our L2GD. However, the performance of FedAvg is not stable but improves with the compression mechanism. The original FedAvg algorithm does not contain any compression mechanism, but for comparison, we incorporated compressors into FedAvg via the following schema which is similar to the classic error feedback Xu et al. (2021a): (i) After local steps, client estimates change of current iterate from the previous round and formulates direction, ${g_{c,\text{computed}}}^i$; ($ii$) client sends compressed difference between previous gradient estimator from previous round and currently computed gradient estimator, $\mathcal{C}({g_{c,\text{computed}}}^i - {g_c}^{i-1})$ to the master; (iii) both master and client updating ${g_c}^i$ via the following schema: ${g_c}^i = {g_c}^{i-1} + \mathcal{C}({g_{c,\text{computed}}}^i - {g_c}^{i-1})$. We provide the details about step size and batch size in Appendix.

7.2.1 Results

We show the results for training `ResNet-18`, `DenseNet-121`, and `MobileNet` with compressed L2GD and other state-of-the-art FL algorithms in Figure 3–5. For these experiments, the communication rounds are set to 12×10^3, 25×10^3, and 20×10^3, respectively. For the FedAvg algorithm, each client performs one epoch over the local data. We empirically tried $1, 2, 3$, and 4 epochs over the local data as local steps, but one epoch is empirically the best choice.

For training `ResNet-18`, from Figure 3 we observe that FedAvg with compression has albeit better convergence than no compression FedAvg [4]. At the same time, compressed FedAvg affects the convergence as a function of communicated rounds only negligibly (see Figure 3 (d),(b)). Therefore, for training other DNN models we use FedAvg with compression and FedOpt without any compressors to enjoy the best of both baselines.

Take away message. Compressed L2GD with natural compressor sends the least data and drives the loss down the most in these experiments. At the same time, L2GD with natural compressor (by design it has smaller variance) reaches the best accuracy for both train and test sets. Compressed L2GD outperforms FedAvg by a huge margin—For all DNN experiments, to reach the desired Top-1 test accuracy, compressed L2GD reduces the communicated data-volume, #bits/n, from 10^{15} to 10^{11}, rendering approximately a 10^4 times improvement compared to FedAvg; see Table 2.

Interestingly, in training `MobileNet`, the performance of biased Top-k compressor degrades only about 10% compared to natural compressor, while approximately degrades 35% in training `DenseNet`. Additionally, see discussion in §A.2, Figures 9–11. This phenomena may lead the researchers to design unbiased compressors with smaller variance to empirically harvest the best behavior of compressed L2GD in personalized FL training.

Nevertheless, we also observe that compressed L2GD converges slower compared to other FL algorithms without compression in all cases. What follows, it can be argued, is that when we compare the communicated data volume for all DNN models, the convergence of compressed L2GD is much better. Additionally, the gain in terms of lowering the loss function value is significant—*by sending the same amount of data, L2GD lowers the loss the most compared to the other no-compression FL baseline algorithms.* These experiments also demonstrate that when communication is a bottleneck, FedAvg is not comparable with L2GD. The only comparable baseline for L2GD is FedOpt; see Table II, also, see discussion in §A.2, Figures 9–11. A similar observation holds for the Top-1 test and train accuracy. Taken together, these indicate that for training larger DNN models in a personalized FL settings, with resource constrained and geographically remote devices, compressed L2GD could be the preferred algorithm because its probabilistic communication protocol sends less data but obtains better test accuracy than no compression FedAvg and FedOpt.

Additionally, we observe that when $\frac{\eta\lambda}{np} \in [0.5, 0.95]$, compressed L2GD incurs a significant variance in objective function during training. Empirically, the best behavior was observed for $\frac{\eta\lambda}{np} \approx 1$ or $\frac{\eta\lambda}{np} \in (0, 0.17]$.

FedAvg as a particular case of L2GD. We note that if $\eta\lambda/np = 1$, then the aggregation step of Algorithm 1 reduces to $x_i^{k+1} = \bar{x}^k$, for all devices. Thus, in this regime L2GD works similarly as FedAvg with random number of local steps. E.g.,if $p = 0.5$, then Algorithm 1 reduces to randomized version of FedAvg with an average of 3 local steps. Figures 6 and 7, confirm this observation numerically, where we see that both algorithms exhibit similar performance. In that experiment we trained `ResNet-56` on `CIFAR10` with $n = 100$ workers, and 600 rounds. For `L2GD`, we set $\frac{\eta\lambda}{pn} = 1$.

8 Conclusion and Future Direction

In this paper, we equipped the loopless gradient descent (L2GD) algorithm with a compression mechanism to reduce the communication bottleneck between local devices and the server in an FL context. We showed that the new algorithm enjoys similar convergence properties as the uncompressed L2GD with a natural increase in the stochastic gradient variance due to compression. This phenomenon is similar to classical convergence bounds for compressed SGD algorithms. We also show that in a personalized FL setting, there is a trade-off that must be considered by devices between learning from other devices' data and spending time learning from their own data. However, a particular parameterization of our algorithm recovers the well-known FedAvg Algorithm. We assessed the performance of the new algorithm compared to the state-of-the-art and validated our theoretical insights through a large set of experiments.

Several questions remain open and merit further investigation in the future. For example, we plan on including compression when devices calculate their local updates, especially in an FL setting, as the devices might not

[4] We have observed that batch normalization Ioffe & Szegedy (2015) in ResNet is sensitive for aggregation; see our discussion in §A.2.

be powerful, and the computing energy is limited, and examine how the algorithm behaves. Additionally, we observed the efficacy of compressed L2GD with a biased compressor, such as Top-k. Nevertheless, extending the compressed L2GD theory for biased compressors (with or without error-feedback Xu et al. (2021a)) is nontrivial and challenging. In the future, we plan to prove a more general theory for compressed L2GD that include both biased and unbiased compressor operating in a bidirectional fashion. A more detailed meta-parameter study covering different network bandwidths, diverse ML tasks with different DNN architectures, and deploying the models on real-life, geographically remote servers will be our future empirical quest.

Acknowledgments

Aritra Dutta acknowledges being an affiliated researcher at the Pioneer Centre for AI, Denmark. The authors acknowledge many fruitful discussions with Md. Patel on this project while he was a remote undergraduate intern at KAUST.

References

Hoefler Alistarh, Konstantinov Johansson, and Renggli Khirirat. The Convergence of Sparsified Gradient Methods. In *NeurIPS*, 2018.

Mohammad Mohammadi Amiri, Deniz Gunduz, Sanjeev R. Kulkarni, and H. Vincent Poor. Federated learning with quantized global model updates. *arXiv:2006.10672*, 2020.

Manoj Ghuhan Arivazhagan, Vinay Aggarwal, Aaditya Kumar Singh, and Sunav Choudhary. Federated learning with personalization layers. *arXiv preprint arXiv:1912.00818*, 2019.

Jeremy Bernstein, Yu-Xiang Wang, Kamyar Azizzadenesheli, and Anima Anandkumar. signSGD: Compressed Optimisation for Non-Convex Problems. In *ICML*, 2018.

Aleksandr Beznosikov, Samuel Horváth, Peter Richtárik, and Mher Safaryan. On biased compression for distributed learning. *arXiv:2002.12410*, 2020.

Simone Bianco, Remi Cadene, Luigi Celona, and Paolo Napoletano. Benchmark analysis of representative deep neural network architectures. *IEEE Access*, 6:64270–64277, 2018.

Keith Bonawitz, Eichner Hubert, Grieskamp Wolfgang, Huba Dzmitry, Ingerman Alex, Ivanov Vladimir, Kiddon Chloe, Konečný Jakub, Mazzocchi Stefano, McMahan H. Brendan, Van Overveldt Timon, Petrou David, Ramage Daniel, and Roselander Jason. Towards federated learning at scale: System design. In *MLSys*, 2019.

C. C. Chang and C. J. Lin. LIBSVM: a library for support vector machines. *ACM Transactions on Intelligent Systems and Technology*, 2011.

Tianyi Chen, Georgios Giannakis, Tao Sun, and Wotao Yin. LAG: Lazily Aggregated Gradient for Communication Efficient Distributed Learning. In *NeurIPS*, 2018a.

Y Chen, Tien-Ju Yang, Joel Emer, and Vivienne Sze. Understanding the limitations of existing energy-efficient design approaches for deep neural networks. *Energy*, 2(L1):L3, 2018b.

Sélim Chraibi, Ahmed Khaled, Dmitry Kovalev, Adil Salim, Peter Richtárik, and Martin Takáč. Distributed fixed point methods with compressed iterates. *arXiv preprint arXiv:1912.09925*, 2019.

Rong Dai, Li Shen, Fengxiang He, Xinmei Tian, and Dacheng Tao. Dispfl: Towards communication-efficient personalized federated learning via decentralized sparse training. In *International Conference on Machine Learning*, 2022.

Alistarh Dan, Grubic Demjan, Li Jerry, Tomioka Ryota, and Vojnovic Milan. QSGD: Communication-Efficient SGD via Gradient Quantization and Encoding. In *NeurIPS*, 2017.

Jeffrey Dean, Greg Corrado, Rajat Monga, Kai Chen, Matthieu Devin, Mark Mao, Marcaurelio Ranzato, Andrew Senior, Paul Tucker, Ke Yang, Quoc Le, and Andrew Ng. Large scale distributed deep networks. In *NeuRIPS*, pp. 1223–1231, 2012.

Yuyang Deng, Mohammad Mahdi Kamani, and Mehrdad Mahdavi. Adaptive personalized federated learning. *arXiv preprint arXiv:2003.13461*, 2020.

A. Dutta, E. Bergou, A. M. Abdelmoniem, C. Y. Ho, A. N. Sahu, M. Canini, and P. Kalnis. On the Discrepancy between the Theoretical Analysis and Practical Implementations of Compressed Communication for Distributed Deep Learning. In *AAAI Conference on Artificial Intelligence*, volume 34, pp. 3817–3824, 2020.

Alireza Fallah, Aryan Mokhtari, and Asuman Ozdaglar. Personalized federated learning with theoretical guarantees: A model-agnostic meta-learning approach. *Advances in Neural Information Processing Systems*, 33:3557–3568, 2020.

Aji Alham Fikri and Heafield Kenneth. Sparse Communication for Distributed Gradient Descent. In *EMNLP-IJCNLP*, 2017.

Rishikesh R Gajjala, Shashwat Banchhor, Ahmed M Abdelmoniem, Aritra Dutta, Marco Canini, and Panos Kalnis. Huffman coding based encoding techniques for fast distributed deep learning. In *Proceedings of ACM CoNEXT's 1st Workshop on Distributed Machine Learning*, pp. 21–27, 2020.

Eva García-Martín, Crefeda Faviola Rodrigues, Graham Riley, and Håkan Grahn. Estimation of energy consumption in machine learning. *Journal of Parallel and Distributed Computing*, 134:75–88, 2019.

Eduard Gorbunov, Filip Hanzely, and Peter Richtárik. Local SGD: unified theory and new efficient methods. In *NeurIPS*, 2020a.

Eduard Gorbunov, Dmitry Kovalev, Dmitry Makarenko, and Peter Richtárik. Linearly converging error compensated SGD. In *NeurIPS*, 2020b.

Robert Mansel Gower, Nicolas Loizou, Xun Qian, Alibek Sailanbayev, Egor Shulgin, and Peter Richtárik. SGD: General analysis and improved rates. In *ICML*, pp. 5200–5209, 2019.

Yunhui Guo. A Survey on Methods and Theories of Quantized Neural Networks. *arXiv:1808.04752v2*, 2018.

Farzin Haddadpour, Mohammad Mahdi Kamani, Mehrdad Mahdavi, and Viveck Cadambe. Trading redundancy for communication: Speeding up distributed sgd for non-convex optimization. In *ICML*, pp. 2545–2554, 2019a.

Farzin Haddadpour, Mohammad Mahdi Kamani, Mehrdad Mahdavi, and Viveck R. Cadambe. Local sgd with periodic averaging: Tighter analysis and adaptive synchronization. In *NeuRIPS*, pp. 11082–11094, 2019b.

F. Hanzely and P. Richtárik. Federated learning of a mixture of global and local models. *arXiv:2002.05516*, 2020.

Chaoyang He, Songze Li, Jinhyun So, Xiao Zeng, Mi Zhang, Hongyi Wang, Xiaoyang Wang, Praneeth Vepakomma, Abhishek Singh, Hang Qiu, et al. Fedml: A research library and benchmark for federated machine learning. *arXiv preprint arXiv:2007.13518*, 2020.

K. He et al. Deep residual learning for image recognition. In *CVPR*, pp. 770–778, 2016.

Mark Horowitz. 1.1 computing's energy problem (and what we can do about it). In *2014 IEEE International Solid-State Circuits Conference Digest of Technical Papers (ISSCC)*, pp. 10–14. IEEE, 2014.

Samuel Horvath, Chen-Yu Ho, Ludovit Horvath, Atal Narayan Sahu, Marco Canini, and Peter Richtárik. Natural Compression for Distributed Deep Learning. *arXiv preprint arXiv:1905.10988v2*, 2019.

Samuel Horváth, Dmitry Kovalev, Konstantin Mishchenko, Sebastian Stich, and Peter Richtárik. Stochastic Distributed Learning with Gradient Quantization and Variance Reduction. *arXiv:1904.05115*, 2019.

Andrew G Howard, Menglong Zhu, Bo Chen, Dmitry Kalenichenko, Weijun Wang, Tobias Weyand, Marco Andreetto, and Hartwig Adam. Mobilenets: Efficient convolutional neural networks for mobile vision applications. *arXiv preprint arXiv:1704.04861*, 2017.

Gao Huang, Zhuang Liu, Laurens van der Maaten, and Kilian Q. Weinberger. Densely Connected Convolutional Networks. In *CVPR*, 2017.

Sergey Ioffe and Christian Szegedy. Batch normalization: Accelerating deep network training by reducing internal covariate shift. In *ICML*, pp. 448–456, 2015.

Martin Jaggi, Virginia Smith, Martin Takac, Jonathan Terhorst, Sanjay Krishnan, Thomas Hofmann, and Michael I Jordan. Communication-Efficient Distributed Dual Coordinate Ascent. In *NeurIPS*, 2014.

Peter Kairouz, H. Brendan McMahan, Brendan Avent, Aurélien Bellet, Mehdi Bennis, Arjun Nitin Bhagoji, Keith Bonawitz, Zachary Charles, Graham Cormode, Rachel Cummings, Rafael G. L. D'Oliveira, Salim El Rouayheb, David Evans, Josh Gardner, Zachary Garrett, Adrià Gascón, Badih Ghazi, Phillip B. Gibbons, Marco Gruteser, Zaid Harchaoui, Chaoyang He, Lie He, Zhouyuan Huo, Ben Hutchinson, Justin Hsu, Martin Jaggi, Tara Javidi, Gauri Joshi, Mikhail Khodak, Jakub Konečný, Aleksandra Korolova, Farinaz Koushanfar, Sanmi Koyejo, Tancrède Lepoint, Yang Liu, Prateek Mittal, Mehryar Mohri, Richard Nock, Ayfer Özgür, Rasmus Pagh, Mariana Raykova, Hang Qi, Daniel Ramage, Ramesh Raskar, Dawn Song, Weikang Song, Sebastian U. Stich, Ziteng Sun, Ananda Theertha Suresh, Florian Tramèr, Praneeth Vepakomma, Jianyu Wang, Li Xiong, Zheng Xu, Qiang Yang, Felix X. Yu, Han Yu, and Sen Zhao. Advances and open problems in federated learning, 2019.

Ahmed Khaled, Konstantin Mishchenko, and Peter Richtárik. First analysis of local GD on heterogeneous data. In *NeurIPS Workshop on Federated Learning for Data Privacy and Confidentiality*, pp. 1–11, 2019.

Ahmed Khaled, Konstantin Mishchenko, and Peter Richtárik. Tighter theory for local SGD on identical and heterogeneous data. In *AISTATS*, pp. 4519–4529, 2020.

Sarit Khirirat, Hamid Reza Feyzmahdavian, and Mikael Johansson. Distributed learning with compressed gradients. *arXiv preprint arXiv:1806.06573*, 2018.

Anastasia Koloskova, Sebastian Stich, and Martin Jaggi. Decentralized Stochastic Optimization and Gossip Algorithms with Compressed Communication. In *ICML*, 2019.

Jakub Konečný and Peter Richtárik. Randomized distributed mean estimation: accuracy vs communication. *Frontiers in Applied Mathematics and Statistics*, 4(62):1–11, 2018.

Jakub Konečný, H. Brendan McMahan, Felix Yu, Peter Richtárik, Ananda Theertha Suresh, and Dave Bacon. Federated learning: Strategies for improving communication efficiency. In *NeuRIPS Workshop on Private Multi-Party Machine Learning*, 2016.

Alex Krizhevsky and Geoffrey Hinton. Learning multiple layers of features from tiny images. Technical Report 0, University of Toronto, Toronto, Ontario, 2009.

Viraj Kulkarni, Milind Kulkarni, and Aniruddha Pant. Survey of personalization techniques for federated learning. In *2020 Fourth World Conference on Smart Trends in Systems, Security and Sustainability (WorldS4)*, pp. 794–797. IEEE, 2020.

Ang Li, Jingwei Sun, Pengcheng Li, Yu Pu, Hai Li, and Yiran Chen. Hermes: an efficient federated learning framework for heterogeneous mobile clients. In *Proceedings of the 27th Annual International Conference on Mobile Computing and Networking*, pp. 420–437, 2021.

Tian Li, Anit Kumar Sahu, Manzil Zaheer, Maziar Sanjabi, Ameet Talwalkar, and Virginia Smith. Federated optimization in heterogeneous networks. In *MLSys*, 2020.

Youjie Li, Mingchao Yu, Songze Li, Salman Avestimehr, Nam Sung Kim, and Alexander Schwing. Pipe-sgd: A decentralized pipelined sgd framework for distributed deep net training. In *NeuRIPS*, pp. 8045–8056, 2018.

Tao Lin, Sebastian U. Stich, Kumar Kshitij Patel, and Martin Jaggi. Don't use large mini-batches, use local sgd. In *ICLR*, 2019.

Xiaosong Ma, Jie Zhang, Song Guo, and Wenchao Xu. Layer-wised model aggregation for personalized federated learning. In *Proceedings of the IEEE/CVF Conference on Computer Vision and Pattern Recognition*, pp. 10092–10101, 2022.

H Brendan McMahan, Eider Moore, Daniel Ramage, Seth Hampson, and Blaise Aguera y Arcas. Communication-efficient learning of deep networks from decentralized data. In *AISTATS*, pp. 1273–1282, 2017.

Yuan Mei, Binbin Guo, Danyang Xiao, and Weigang Wu. Fedvf: Personalized federated learning based on layer-wise parameter updates with variable frequency. In *2021 IEEE International Performance, Computing, and Communications Conference (IPCCC)*, pp. 1–9, 2021.

Konstantin Mishchenko, Ahmed Khaled Ragab Bayoumi, and Peter Richtárik. Random reshuffling: Simple analysis with vast improvements. In *NeurIPS*, volume 33, 2020.

Constantin Philippenko and Aymeric Dieuleveut. Artemis: tight convergence guarantees for bidirectional compression in federated learning. *arXiv:2006.14591*, 2020.

Krishna Pillutla, Kshitiz Malik, Abdel-Rahman Mohamed, Mike Rabbat, Maziar Sanjabi, and Lin Xiao. Federated learning with partial model personalization. In *International Conference on Machine Learning*, pp. 17716–17758, 2022.

Sashank Reddi, Zachary Charles, Manzil Zaheer, Zachary Garrett, Keith Rush, Jakub Konečnỳ, Sanjiv Kumar, and H Brendan McMahan. Adaptive federated optimization. *arXiv preprint arXiv:2003.00295*, 2020.

Amirhossein Reisizadeh, Aryan Mokhtari, Hamed Hassani, Ali Jadbabaie, and Ramtin Pedarsani. Fedpaq: A communication-efficient federated learning method with periodic averaging and quantization. In *AISTATS*, pp. 2021–2031, 2020.

Mher Safaryan, Egor Shulgin, and Peter Richtárik. Uncertainty principle for communication compression in distributed and federated learning and the search for an optimal compressor. *Information and Inference: A Journal of the IMA*, 2021.

Atal Sahu, Aritra Dutta, Ahmed M Abdelmoniem, Trambak Banerjee, Marco Canini, and Panos Kalnis. Rethinking gradient sparsification as total error minimization. *Advances in Neural Information Processing Systems*, 34:8133–8146, 2021.

Ohad Shamir, Nati Srebro, and Tong Zhang. Communication-Efficient Distributed Optimization using an Approximate Newton-type Method. In *ICML*, 2014.

Aviv Shamsian, Aviv Navon, Ethan Fetaya, and Gal Chechik. Personalized federated learning using hypernetworks. In *International Conference on Machine Learning*, pp. 9489–9502. PMLR, 2021.

Yiqing Shen, Yuyin Zhou, and Lequan Yu. Cd2-pfed: Cyclic distillation-guided channel decoupling for model personalization in federated learning. In *Proceedings of the IEEE/CVF Conference on Computer Vision and Pattern Recognition*, pp. 10041–10050, 2022.

N. Shlezinger, Mingzhe Chen, Yonina Eldar, and H. Vincent Poor. Federated learning with quantization constraints. In *ICASSP*, pp. 8851–8855, 2020.

Virginia Smith, Chao-Kai Chiang, Maziar Sanjabi, and Ameet Talwalkar. Federated multi-task learning. In *NeuRIPS*, pp. 4424–4434, 2017.

Sebastian U. Stich. Local SGD converges fast and communicates little. In *ICLR*, 2019.

Sebastian U Stich, Jean-Baptiste Cordonnier, and Martin Jaggi. Sparsified SGD with Memory. In *NeurIPS*, 2018.

N. Strom. Scalable distributed DNN training using commodity GPU cloud computing. In *INTERSPEECH*, pp. 1488–1492, 2015.

Ananda Theertha Suresh, Felix X. Yu, Sanjiv Kumar, and H. Brendan McMahan. Distributed mean estimation with limited communication. In *ICML*, 2017.

Alysa Ziying Tan, Han Yu, Lizhen Cui, and Qiang Yang. Towards personalized federated learning. *IEEE Transactions on Neural Networks and Learning Systems*, 2022.

Hanlin Tang, Chen Yu, Xiangru Lian, Tong Zhang, and Ji Liu. DoubleSqueeze: Parallel Stochastic Gradient Descent with Double-pass Error-Compensated Compression. In *ICML*, 2019.

Thijs Vogels, Sai Praneeth Karimireddy, and Martin Jaggi. PowerSGD: Practical Low-Rank Gradient Compression for Distributed Optimization. In *NeurIPS*, 2019.

H. Wang et al. ATOMO: Communication-efficient Learning via Atomic Sparsification. In *NeuRIPS*, pp. 9850–9861. 2018.

Jianyu Wang and Gauri Joshi. Adaptive Communication Strategies to Achieve the Best Error-Runtime Trade-off in Local-Update SGD. In *MLSys*, 2019.

W. Wen et al. Terngrad: Ternary gradients to reduce communication in distributed deep learning. In *NeuRIPS*, pp. 1508–1518, 2017.

Jiaxiang Wu, Weidong Huang, Junzhou Huang, and Tong Zhang. Error Compensated Quantized SGD and its Applications to Large-scale Distributed Optimization. In *ICML*, 2018.

Hang Xu, Chen-Yu Ho, Ahmed M Abdelmoniem, Aritra Dutta, El Houcine Bergou, Konstantinos Karatsenidis, Marco Canini, and Panos Kalnis. GRACE: A Compressed Communication Framework for Distributed Machine Learning. In *2021 IEEE 41st International Conference on Distributed Computing Systems (ICDCS)*, pp. 561–572, 2021a.

Hang Xu, Kelly Kostopoulou, Aritra Dutta, Xin Li, Alexandros Ntoulas, and Panos Kalnis. Deepreduce: A sparse-tensor communication framework for federated deep learning. *Advances in Neural Information Processing Systems*, 34:21150–21163, 2021b.

Hao Yu, Rong Jin, and Sen Yang. On the Linear Speedup Analysis of Communication Efficient Momentum SGD for Distributed Non-Convex Optimization. In *ICML*, 2019a.

Yue Yu, Jiaxiang Wu, and Junzhou Huang. Exploring Fast and Communication-Efficient Algorithms in Large-Scale Distributed Networks. In *AISTATS*, 2019b.

Hantian Zhang, Jerry Li, Kaan Kara, Dan Alistarh, Ji Liu, and Ce Zhang. ZipML: Training Linear Models with End-to-End Low Precision, and a Little Bit of Deep Learning. In *ICML*, 2017.

Michael Zhang, Karan Sapra, Sanja Fidler, Serena Yeung, and Jose M. Alvarez. Personalized federated learning with first order model optimization. In *International Conference on Learning Representations*, 2021.

Sixin Zhang, Anna Choromanska, and Yann LeCun. Deep learning with elastic averaging sgd. In *NeuRIPS*, pp. 685–693, 2015.

Fan Zhou and Guojing Cong. On the convergence properties of a k-step averaging stochastic gradient descent algorithm for nonconvex optimization. In *IJCAI*, pp. 3219–3227, 2018.

A Appendix

A.1 Convergence Analysis—Proofs of the Lemmas and the Theorems

In this section, we provide the proofs of convex and non-convex convergence results of the compressed L2GD algorithm.

Overview of results. In §A.1.1, we provide the technical lemmas necessary for the analyses. §A.1.2 contains the auxiliary results pertaining to both convex and nonconvex convergence. In §A.1.3 we provide the non-convex convergence results, and §A.1.4 provides the proofs for optimal rate and communication.

A.1.1 Technical results used for convergence

The following two Lemmas are instrumental in proving other compression related results.

Lemma 1 *Let $x \in R^{nd}$, then*

$$\mathbb{E}_{\mathcal{C}}\left[\|\mathcal{C}(x)\|^2\right] \leq (1+\omega)\|x\|^2,$$

where $\omega = \max_{i=1,\ldots,n}\{\omega_i\}$.

Proof 2 *By using Assumption 1, we have*

$$\mathbb{E}_{\mathcal{C}}\left[\|\mathcal{C}(x)\|^2\right] = \mathbb{E}_{\mathcal{C}}\left[\sum_{i=1}^{n}\|\mathcal{C}_i(x_i)\|^2\right] = \sum_{i=1}^{n}\mathbb{E}_{\mathcal{C}_i}\|\mathcal{C}_i(x_i)\|^2 \leq \sum_{i=1}^{n}(1+\omega_i)\|x_i\|^2 \leq (1+\omega)\|x\|^2.$$

Hence the result.

Lemma 2 *Let Assumption 1 hold, then for all $k \geq 0$, $\mathbb{E}_{\mathcal{C},\mathcal{C}_M}\left[\mathcal{C}_M(\bar{y}^k)\right] = \bar{x}^k$.*

Proof 3 *We have*

$$\mathbb{E}_{\mathcal{C},\mathcal{C}_M}\left[\mathcal{C}_M(\bar{y}^k)\right] = \mathbb{E}_{\mathcal{C}}\left[\mathbb{E}_{\mathcal{C}_M}\left[\mathcal{C}_M(\bar{y}^k)\right]\right] = \mathbb{E}_{\mathcal{C}}\left[\frac{1}{n}\sum_{j=1}^{n}\mathcal{C}_j(x_j^k)\right] = \frac{1}{n}\sum_{j=1}^{n}\mathbb{E}_{\mathcal{C}_j}\left[\mathcal{C}_j(x_j^k)\right] = \bar{x}^k.$$

Hence the result.

In the following Lemma, we show that based on the randomness of the compression operators, in expectation, we recover the exact average of the local models and the exact gradient for all iterations.

Lemma 3 *Let Assumptions 1 hold. Then for all $k \geq 0$, knowing x^k, $G(x^k)$ is an unbiased estimator of the gradient of function F at x^k.*

Proof 4 *We have*

$$\mathbb{E}_{\mathcal{C},\mathcal{C}_M}\left[G_i(x^k)\right] = \begin{cases} \frac{\nabla f_i(x_i^k)}{n(1-p)} & \text{if } \xi_k = 0 \\ \frac{\lambda}{np}\left(x_i^k - \mathbb{E}_{C,\mathcal{C}_M}\left[\mathcal{C}_M(\bar{y}^k)\right]\right) & \text{if } \xi_k = 1 \ \&\ \xi_{k-1} = 0, \\ \frac{\lambda}{np}\left(x_i^k - \bar{x}^k\right) & \text{if } \xi_k = 1 \ \&\ \xi_{k-1} = 1, \end{cases}$$

$$\overset{\text{By Lemma 2}}{=} \begin{cases} \frac{\nabla f_i(x_i^k)}{n(1-p)} & \text{if } \xi_k = 0, \\ \frac{\lambda}{np}\left(x_i^k - \bar{x}^k\right) & \text{if } \xi_k = 1. \end{cases}$$

Therefore,

$$\begin{aligned} \mathbb{E}[G_i(x^k)|x^k] &= \mathbb{E}_{\xi_k}\left[\mathbb{E}_{C,\mathcal{C}_M}\left[G_i(x^k)\right]\right] \\ &= (1-p)\frac{\nabla f_i(x_i^k)}{n(1-p)} + p\frac{\lambda}{np}\left(x_i^k - \bar{x}^k\right) \\ &= \nabla_{x_i} f(x^k) + \nabla_{x_i} h\left(x^k\right) = \nabla_{x_i} F(x^k). \end{aligned}$$

Hence the result.

A.1.2 Main convergence results

Based on the results given in the previous section, we are now set to quote our key convergence results. Our next lemma gives an upper bound on the iterate at each iteration. This bound is composed of two terms—the optimality gap, $F(x^k) - F(x^*)$, and the norm of the optimal point, $\|x^*\|$.

Lemma 4 *Let Assumption 2 hold, then*

$$\left\|x^k\right\|^2 \leq \tfrac{4}{\mu}\left(F(x^k) - F(x^*)\right) + 2\left\|x^*\right\|^2.$$

Proof 5 *We have*

$$\left\|x^k\right\|^2 \overset{\|a+b\|^2 \leq 2\|a\|^2 + 2\|b\|^2}{\leq} 2\left\|x^k - x^*\right\|^2 + 2\left\|x^*\right\|^2 \leq \frac{4}{\mu}\left(F(x^k) - F(x^*)\right) + 2\left\|x^*\right\|^2.$$

Hence the result.

Recall that, inspired by the expected smoothness property Gower et al. (2019), we use a similar idea in our convergence proofs. The next lemma is a technical Lemma that helps us to prove the expected smoothness property Gower et al. (2019). The bound in Lemma 5 is composed of the optimality gap, $F(x^k) - F(x^*)$, the difference between the gradients of h at x^k and x^*, that is, $\left\|\nabla h(x^k) - \nabla h(x^*)\right\|$, and an extra constant, β, which depends on the used compressors.

Lemma 5 *Let Assumptions 1 and 2 hold, then*

$$\mathcal{A} := \mathbb{E}_{\mathcal{C}_M,\mathcal{C}}\left\|x^k - Q\mathcal{C}_M(\bar{y}^k) - x^* + Q\mathcal{C}_M(\bar{y}^*)\right\|^2 \leq \tfrac{4n^2}{\lambda^2}\left\|\nabla h(x^k) - \nabla h(x^*)\right\|^2 + \alpha\left(F(x^k) - F(x^*)\right) + \beta,$$

where $\bar{y}^* := \frac{1}{n}\sum_{j=1}^n \mathcal{C}_j(x_j^*)$, $\alpha := \frac{4(4\omega + 4\omega_M(1+\omega))}{\mu}$, *and*

$$\beta := 2\left(4\omega + 4\omega_M(1+\omega)\right)\left\|x^*\right\|^2 + 4\mathbb{E}_{\mathcal{C}_M,\mathcal{C}}\left\|Q\mathcal{C}_M(\bar{y}^*) - Q\bar{x}^*\right\|^2.$$

Proof 6 *We have*

$$\begin{aligned}
\mathcal{A} &= \mathbb{E}_{\mathcal{C}_M,\mathcal{C}}\left\|x^k - Q\bar{x}^k + Q\bar{x}^k - Q\mathcal{C}_M(\bar{y}^k) - x^* + Q\bar{x}^* - Q\bar{x}^* + Q\mathcal{C}_M(\bar{y}^*)\right\|^2 \\
&= \mathbb{E}_{\mathcal{C}_M,\mathcal{C}}\left\|\left(x^k - Q\bar{x}^k - x^* + Q\bar{x}^*\right) + \left(Q\bar{x}^k - Q\bar{y}^k\right) + \left(Q\bar{y}^k - Q\mathcal{C}_M(\bar{y}^k)\right) + \left(Q\mathcal{C}_M(\bar{y}^*) - Q\bar{x}^*\right)\right\|^2 \\
&\leq 4\left\|x^k - Q\bar{x}^k - x^* + Q\bar{x}^*\right\|^2 + 4\mathbb{E}_{\mathcal{C}}\left\|Q\bar{x}^k - Q\bar{y}^k\right\|^2 + 4\mathbb{E}_{\mathcal{C}_M,\mathcal{C}}\left\|Q\bar{y}^k - Q\mathcal{C}_M(\bar{y}^k)\right\|^2 \\
&+ 4\mathbb{E}_{\mathcal{C}_M,\mathcal{C}}\left\|Q\mathcal{C}_M(\bar{y}^*) - Q\bar{x}^*\right\|^2 \\
&= 4\left\|x^k - Q\bar{x}^k - x^* + Q\bar{x}^*\right\|^2 + 4n\mathbb{E}_{\mathcal{C}}\left\|\bar{x}^k - \bar{y}^k\right\|^2 + 4n\mathbb{E}_{\mathcal{C}_M,\mathcal{C}}\left\|\bar{y}^k - \mathcal{C}_M(\bar{y}^k)\right\|^2 \\
&+ 4\mathbb{E}_{\mathcal{C}_M,\mathcal{C}}\left\|Q\mathcal{C}_M(\bar{y}^*) - Q\bar{x}^*\right\|^2 \\
&\leq 4\left\|x^k - Q\bar{x}^k - x^* + Q\bar{x}^*\right\|^2 + 4\sum_{i=1}^n \mathbb{E}_{\mathcal{C}}\left\|x_i^k - \mathcal{C}_i(x_i^k)\right\|^2 + 4n\omega_M\mathbb{E}_{\mathcal{C}_M}\left\|\bar{y}^k\right\|^2 \\
&+ 4\mathbb{E}_{\mathcal{C}_M,\mathcal{C}}\left\|Q\mathcal{C}_M(\bar{y}^*) - Q\bar{x}^*\right\|^2 \\
&\leq 4\left\|x^k - Q\bar{x}^k - x^* + Q\bar{x}^*\right\|^2 + 4\sum_{i=1}^n \omega_i\left\|x_i^k\right\|^2 + 4\omega_M\sum_{i=1}^n(1+\omega_i)\left\|x_i^k\right\|^2 + 4\mathbb{E}_{\mathcal{C}_M,\mathcal{C}}\left\|Q\mathcal{C}_M(\bar{y}^*) - Q\bar{x}^*\right\|^2 \\
&\leq 4\frac{n^2}{\lambda^2}\left\|\nabla h(x^k) - \nabla h(x^*)\right\|^2 + \left(4\omega + 4\omega_M(1+\omega)\right)\left\|x^k\right\|^2 + 4\mathbb{E}_{\mathcal{C}_M,\mathcal{C}}\left\|Q\mathcal{C}_M(\bar{y}^*) - Q\bar{x}^*\right\|^2 \\
&\overset{\text{By Lemma 4}}{\leq} 4\frac{n^2}{\lambda^2}\left\|\nabla h(x^k) - \nabla h(x^*)\right\|^2 + \left(4\omega + 4\omega_M(1+\omega)\right)\left(\frac{4}{\mu}\left(F(x^k) - F(x^*)\right) + 2\left\|x^*\right\|^2\right) \\
&\quad + 4\mathbb{E}_{\mathcal{C}_M,\mathcal{C}}\left\|Q\mathcal{C}_M(\bar{y}^*) - Q\bar{x}^*\right\|^2 \\
&\leq 4\frac{n^2}{\lambda^2}\left\|\nabla h(x^k) - \nabla h(x^*)\right\|^2 + \alpha\left(F(x^k) - F(x^*)\right) + \beta.
\end{aligned}$$

Hence the result.

Now we are all set to prove the expected smoothness property in our setup.

Lemma 6 (Expected Smoothness) *Let Assumptions 1 and 2 hold, then*

$$\mathbb{E}\left[\|G(x^k)\|^2|x^k\right] \leq 4\gamma\left(F(x^k)-F(x^*)\right)+\delta, \tag{3}$$

where

$$\gamma := \frac{\alpha\lambda^2(1-p)}{2n^2p}+\max\left\{\frac{L_f}{(1-p)},\frac{\lambda}{n}\left(1+\frac{4(1-p)}{p}\right)\right\}$$

and

$$\delta := \frac{2\beta\lambda^2(1-p)}{n^2p}+2\mathbb{E}\|G(x^*)\|^2.$$

Proof 7 *We have*

$$\|G(x^k)-G(x^*)\|^2 = \begin{cases} \frac{\|\nabla f\left(x^k\right)-\nabla f(x^*)\|^2}{(1-p)^2} & \text{if } \xi_k=0 \\ \frac{\lambda^2}{n^2p^2}\left\|x^k-Q\mathcal{C}_M(\bar{y}^k)-x^*+Q\mathcal{C}_M(\bar{y}^*)\right\|^2 & \text{if } \xi_k=1 \ \&\ \xi_{k-1}=0, \\ \frac{1}{p^2}\|\nabla h(x^k)-\nabla h(x^*)\|^2 & \text{if } \xi_k=1 \ \&\ \xi_{k-1}=1. \end{cases}$$

Finally,

$$\begin{aligned}
\mathbb{E}_{\xi_k,\xi_{k-1}}\|G(x^k)-G(x^*)\|^2 &= (1-p)\frac{\|\nabla f\left(x^k\right)-\nabla f\left(x^*\right)\|^2}{(1-p)^2}+p^2\frac{1}{p^2}\|\nabla h(x^k)-\nabla h(x^*)\|^2 \\
&+ p(1-p)\frac{\lambda^2}{n^2p^2}\left\|x^k-Q\mathcal{C}_M(\bar{y}^k)-x^*+Q\mathcal{C}_M(\bar{y}^*)\right\|^2 \\
&= \frac{\|\nabla f\left(x^k\right)-\nabla f\left(x^*\right)\|^2}{(1-p)}+\|\nabla h(x^k)-\nabla h(x^*)\|^2 \\
&+ \frac{\lambda^2(1-p)}{n^2p}\left\|x^k-Q\mathcal{C}_M(\bar{y}^k)-x^*+Q\mathcal{C}_M(\bar{y}^*)\right\|^2.
\end{aligned}$$

Therefore, by using Lemma 5 we get

$$\begin{aligned}
\mathbb{E}\|G(x^k)-G(x^*)|x^k\|^2 &= \frac{\|\nabla f\left(x^k\right)-\nabla f\left(x^*\right)\|^2}{(1-p)}+\|\nabla h(x^k)-\nabla h(x^*)\|^2+\frac{\lambda^2(1-p)}{n^2p}\mathcal{A} \\
&\leq \frac{\|\nabla f\left(x^k\right)-\nabla f\left(x^*\right)\|^2}{(1-p)}+\|\nabla h(x^k)-\nabla h(x^*)\|^2 \\
&+ \frac{\lambda^2(1-p)}{n^2p}\left(4\frac{n^2}{\lambda^2}\left\|\nabla h(x^k)-\nabla h(x^*)\right\|^2+\alpha\left(F(x^k)-F(x^*)\right)+\beta\right) \\
&= \frac{\|\nabla f\left(x^k\right)-\nabla f\left(x^*\right)\|^2}{(1-p)}+\left(1+\frac{4(1-p)}{p}\right)\|\nabla h(x^k)-\nabla h(x^*)\|^2 \\
&+ \frac{\alpha\lambda^2(1-p)}{n^2p}\left(F(x^k)-F(x^*)\right)+\frac{\beta\lambda^2(1-p)}{n^2p} \\
&\leq \frac{2L_f}{(1-p)}\left(f(x^k)-f(x^*)\right)+\frac{2\lambda}{n}\left(1+\frac{4(1-p)}{p}\right)\left(h(x^k)-h(x^*)\right) \\
&+ \frac{\alpha\lambda^2(1-p)}{n^2p}\left(F(x^k)-F(x^*)\right)+\frac{\beta\lambda^2(1-p)}{n^2p} \\
&\leq 2\gamma\left(F(x^k)-F(x^*)\right)+\frac{\beta\lambda^2(1-p)}{n^2p}.
\end{aligned}$$

Finally, we obtain

$$\begin{aligned}
\mathbb{E}\|G(x^k)|x^k\|^2 &\leq 2\mathbb{E}\|G(x^k)-G(x^*)|x^k\|^2+2\mathbb{E}\|G(x^*)\|^2 \\
&\leq 4\gamma\left(F(x^k)-F(x^*)\right)+\frac{2\beta\lambda^2(1-p)}{n^2p}+2\mathbb{E}\|G(x^*)\|^2 \\
&\leq 4\gamma\left(F(x^k)-F(x^*)\right)+\delta.
\end{aligned}$$

Hence the result.

Based on the above results, the convergence of Algorithm 1 for strongly convex functions follows directly from Lemmas 3, 6 and Theorem 3.1 from Gower et al. (2019).

A.1.3 Nonconvex convergence

To prove the convergence of Algorithm 1 for L-smooth, nonconvex functions we need an addtional result. The next Lemma from Mishchenko et al. (2020) is a key lemma to prove the convergence of nonconvex case. Our proof of the lemma is different from Mishchenko et al. (2020).

Lemma 8 *Let for $0 \leq k \leq K$ the following holds:*

$$p_{k+1} \leq (1+a)p_k - bq_k + c, \tag{4}$$

where $\{p_k\}_{k=0}^K$ and $\{q_k\}_{k=0}^K$ are non-negative sequences and $a, b, c \geq 0$ are constants. Then

$$\min_{k=0,1,\cdots K-1} q_k \leq \frac{(1+a)^K}{bK} p_0 + \frac{c}{b}. \tag{5}$$

Proof 8 *Dividing both sides of equation 4 by $(1+a)^{K+1}$ and summing from $k = 0, 1, \cdots K$ we have*

$$\sum_{k=0}^{K} \frac{1}{(1+a)^{K+1}} p_{k+1} \leq \sum_{k=0}^{K} \frac{1}{(1+a)^K} p_k - \sum_{k=0}^{K} \frac{b}{(1+a)^{K+1}} q_k + \sum_{k=0}^{K} \frac{c}{(1+a)^{K+1}}. \tag{6}$$

After rearranging it becomes

$$\sum_{k=0}^{K} \frac{b}{(1+a)^{K+1}} q_k \leq p_0 - \frac{1}{(1+a)^{K+1}} p_{K+1} + \sum_{k=0}^{K} \frac{c}{(1+a)^{K+1}}. \tag{7}$$

Noting $\sum_{k=0}^{K} \frac{1}{(1+a)^{K+1}} \leq \frac{1}{1-\frac{1}{1+a}} - 1 = \frac{1}{a}$, we have

$$\min_{k=0,1,\cdots K} q_k \sum_{k=0}^{K} \frac{1}{(1+a)^{K+1}} \leq \sum_{k=0}^{K} \frac{1}{(1+a)^{K+1}} q_k \leq \frac{p_0}{b} + \frac{c}{ab}. \tag{8}$$

Hence the result.

Now we are all set to prove the nonconvex convergence result.

Theorem 5 (Non convex case) *Let Assumption 1 hold. Assume also that F is L-smooth, bounded from below by $F(x^*)$. Then to reach a precision, $\epsilon > 0$, set the stepsize, $\eta = \min\{\frac{1}{\sqrt{2L\gamma K}}, \frac{\epsilon^2}{L\delta}\}$, such that for $K \geq \frac{6L}{\epsilon^4} \max\{12\gamma(F(x^0) - F(x^*))^2, \delta\}$, we have $\min_{k=0,1,\ldots,K} \mathbb{E}\|\nabla F(x^k)\|_2 \leq \epsilon$.*

Proof 9 *From L-smoothness of F we have*

$$F(x^{k+1}) \quad \leq \quad F(x^k) - \eta_k \boldsymbol{e} \nabla F(x^k) G(x^k) + \frac{L}{2} \eta_k^2 \|G(x_k)\|^2.$$

By taking the expectation in the above inequality, conditional on x^k, we get

$$\mathbb{E}\left[F(x^{k+1}) \mid x^k\right] \overset{\text{By Lemma 3}}{\leq} F(x^k) - \eta_k \|\nabla F(x^k)\|_2^2 + \frac{L\eta_k^2}{2} \mathbb{E}\left(\|G(x_k)\|^2 | x_k\right),$$

which by using Lemma 6 reduces to

$$\begin{aligned} \mathbb{E}\left[F(x^{k+1}) \mid x^k\right] &\leq F(x^k) - \eta_k \|\nabla F(x^k)\|_2^2 + \frac{L\eta_k^2}{2} \left(4\gamma \left(F(x^k) - F(x^*)\right) + \delta\right) \\ &\leq F(x^k) - \eta_k \|\nabla F(x^k)\|_2^2 + 2L\eta_k^2 \gamma \left(F(x^k) - F(x^*)\right) + \frac{L\eta_k^2 \delta}{2}. \end{aligned}$$

By taking the expectation in the last inequality, we get

$$\mathbb{E}\big[F(x^{k+1})\big] - F(x^*) \quad \leq \quad (1 + 2L\eta_k^2\gamma)\left(\mathbb{E}\big[F(x^k)\big] - F(x^*)\right) - \eta_k \mathbb{E}\|\nabla F(x^k)\|_2^2 + \frac{L\eta_k^2\delta}{2}. \tag{9}$$

Consider $\eta_k = \eta > 0$ in equation 9. Then, equation equation 9 is similar to equation 4 with $p_k = \mathbb{E}\big[F(x^k)\big] - F(x^*), q_k = \mathbb{E}\|\nabla F_k\|^2, a = 2L\gamma\eta^2, b = \eta, c = \frac{L\eta^2\delta}{2}$. Therefore,

$$\min_{k=0,1,\cdots K-1} \mathbb{E}\|\nabla F(x^k)\|^2 \quad \leq \quad \frac{(1 + 2L\gamma\eta^2)^K}{\eta K}\left(F(x^0) - F(x^*)\right) + \frac{L\eta\delta}{2}. \tag{10}$$

Now setting η such that $2L\gamma\eta^2 K \leq 1$, and the inequality, $(1+x)^K \leq e^{xK}$ we have

$$\min_{k=0,1,\cdots K-1} \mathbb{E}\|\nabla F(x^k)\|^2 \quad \leq \quad \frac{3\left(F(x^0) - F(x^*)\right)}{\eta K} + \frac{L\eta\delta}{2}. \tag{11}$$

For a given precision, $\epsilon > 0$, to make $\min_{k=0,1,\cdots K-1} \mathbb{E}\|\nabla F(x^k)\|^2 \leq \epsilon^2$, we require $\frac{3\left(F(x^0)-F(x^*)\right)}{\eta K} \leq \frac{\epsilon^2}{2}$ and $L\eta\delta \leq \epsilon^2$, resulting in

$$K \geq \frac{6(F(x^0) - F(x^*))}{\eta\epsilon^2} \text{ and } \eta \leq \frac{\epsilon^2}{L\delta}.$$

The above, alongwith $\eta \leq \frac{1}{\sqrt{2L\gamma K}}$, implies

$$K \geq \frac{72L\gamma(F(x^0) - F(x^*))^2}{\epsilon^4} \text{ and } K \geq \frac{6L\delta}{\epsilon^4}.$$

Hence the result.

A.1.4 Optimal rate and communication

The following proofs are related to optimal rate and communication as given in §6.

Theorem 1 (Optimal rate) *The probability p^* minimizing γ is equal to $\max\{p_e, p_A\}$, where $p_e = \frac{7\lambda+L-\sqrt{\lambda^2+14\lambda L+L^2}}{6\lambda}$ and p_A is the optimizer of the function $A(p) = \frac{\alpha\lambda^2}{2n^2p} + \frac{L}{n(1-p)}$ in $(0,1)$.*

Proof 10 *We can rewrite γ as follows*

$$\gamma \quad = \quad -\frac{\alpha\lambda^2}{2n^2} + \max\left\{A(p), B(p)\right\},$$

where $A(p) = \frac{\alpha\lambda^2}{2n^2p} + \frac{L}{n(1-p)}$ and $B(p) = \frac{\alpha\lambda^2}{2n^2p} + \frac{4\lambda}{np} - \frac{3\lambda}{n}$. The function B is monotonically decreasing as a function of p. The function A goes to ∞ as p goes to zero or one, and it has one stationary point between zero and one hence it is convex in the interval $(0,1)$. Thus it admits an optimizer p_A in $(0,1)$. Note that $p_e = \frac{7\lambda+L-\sqrt{\lambda^2+14\lambda L+L^2}}{6\lambda}$ is the point for which $A(p)$ is equal to $B(p)$. Note also that near to zero $B(p) \geq A(p)$. Therefore if $p_e \leq p_A$ then the optimizer of γ is p_A otherwise it is equal to p_e. Thus the probability p^* optimizing γ is equal to $\max\{p_e, p_A\}$.

Lemma 7 *The optimizer probability p_A of the function $A(p) = \frac{\alpha\lambda^2}{2n^2p} + \frac{L}{n(1-p)}$ in $(0,1)$ is equal to*

$$p_A = \begin{cases} \frac{1}{2} & \text{if } 2nL = \alpha\lambda^2 \\ \frac{-2\alpha\lambda^2+2\lambda\sqrt{2\alpha nL}}{2(2nL-\alpha\lambda^2)} & \text{if } 2nL > \alpha\lambda^2 \\ \frac{-2\alpha\lambda^2-2\lambda\sqrt{2\alpha nL}}{2(2nL-\alpha\lambda^2)} & \text{otherwise} \end{cases}$$

Proof 11 *If $2nL \neq \alpha\lambda^2$, then the function A has the following two stationary points $\frac{-2\alpha\lambda^2+2\lambda\sqrt{2\alpha nL}}{2(2nL-\alpha\lambda^2)}$ and $\frac{-2\alpha\lambda^2-2\lambda\sqrt{2\alpha nL}}{2(2nL-\alpha\lambda^2)}$. If $2nL = \alpha\lambda^2$, then the function A has one stationary point equal to $\frac{1}{2}$.*

Theorem 2 (Optimal communication) *The probability p^* optimizing C is equal to $\max\{p_e, p_A\}$, where $p_e = \frac{7\lambda+L-\sqrt{\lambda^2+14\lambda L+L^2}}{6\lambda}$ and $p_A = 1 - \frac{Ln}{\alpha\lambda^2}$.*

Proof 12 *We can rewrite nC as follows*

$$nC \quad = \quad \max\left\{A(p), B(p)\right\},$$

where $A(p) = \frac{\alpha\lambda^2 p(1-p)}{2n} + \frac{\alpha\lambda^2(1-p)}{2n} + Lp$ and $B(p) = \frac{\alpha\lambda^2 p(1-p)}{2n} + \frac{\alpha\lambda^2(1-p)}{2n} + 4\lambda(1-p) - 3\lambda p(1-p)$. The function B is monotonically decreasing as a function of p in $[0,1]$. Note that $B(0) = \frac{\alpha\lambda^2}{2n} + 4\lambda$ and $B(1) = 0$. The function A admits a minimizer equal to $p_A = 1 - \frac{Ln}{\alpha\lambda^2}$. Of course p_A is a probability under the condition that $Ln \leq \alpha\lambda^2$. Thus we consider the following 2 scenarios

1. *If $Ln > \alpha\lambda^2$ ($p_A < 0$) then $p^* = p_e$*
2. *else $p^* = \max\{p_e, p_A\}$.*

We conclude in both cases that $p^* = \max\{p_e, p_A\}$.

A.2 Addendum to the Experimental Results

Batch Normalization. Beside the trainable parameters, the ResNet models contain batch normalization Ioffe & Szegedy (2015) layers that are crucial for training. The logic of batch normalization depends on the estimation of running mean and variance, and these statistics can be pretty personalized for each client in a heterogeneous data regime. The implementation of FedAvg and FedOpt in FedML considers the averaging of these statistics during the aggregation phase. In our implementation, the batch normalization statistics are included into aggregation.

Step-size. The step-sizes for FedAvg and FedOpt tuned via selecting step sizes from the following set $\{0.01, 0.1, 0.2, 0.5, 1.0, 2.0, 4.0\}$. We consider the step size for both algorithms to be 0.1. Starting with step size 0.2 algorithms diverge; we also did not use use step size schedulers. Additionally, we have tuned number of local epochs for FedAvg from the following set $\{1, 2, 3, 4\}$. The used batch size is set to 256.

Compressed L2Gd vs. FedOpt. From the experiments in Section 7.2, Figures 3–5, we realized that FedAvg is not a competitive no-compression baseline for L2GD; see Table 2. FedOpt, on the other hand, remains a competitive no-compression baseline comparable to compressed L2GD. Therefore, we separately measure the performance of compressed L2GD and non-compression FedOpt for training `ResNet-18`, `DenseNet-121`, and `MobileNet`. Figures 8–9 demonstrate that L2GD with natural compressor (that by design has small variance) empirically behaves the best and converges approximately 5 times faster compare to FedOpt. They also show that compressed L2GD with natural compressor sends the least data and drives the loss down the most. At the same time, L2GD with natural compressor reaches the best accuracy for both train and test sets.

Reproducible research. See our repository online: `https://github.com/burlachenkok/compressed-fl-l2gd-code`. Our source codes have been constructed on top of the following version of FedML.ai: `https://github.com/FedML-AI/FedML/commit/3b9b68764d922ce239e0b84aceda986cfa977f96`.

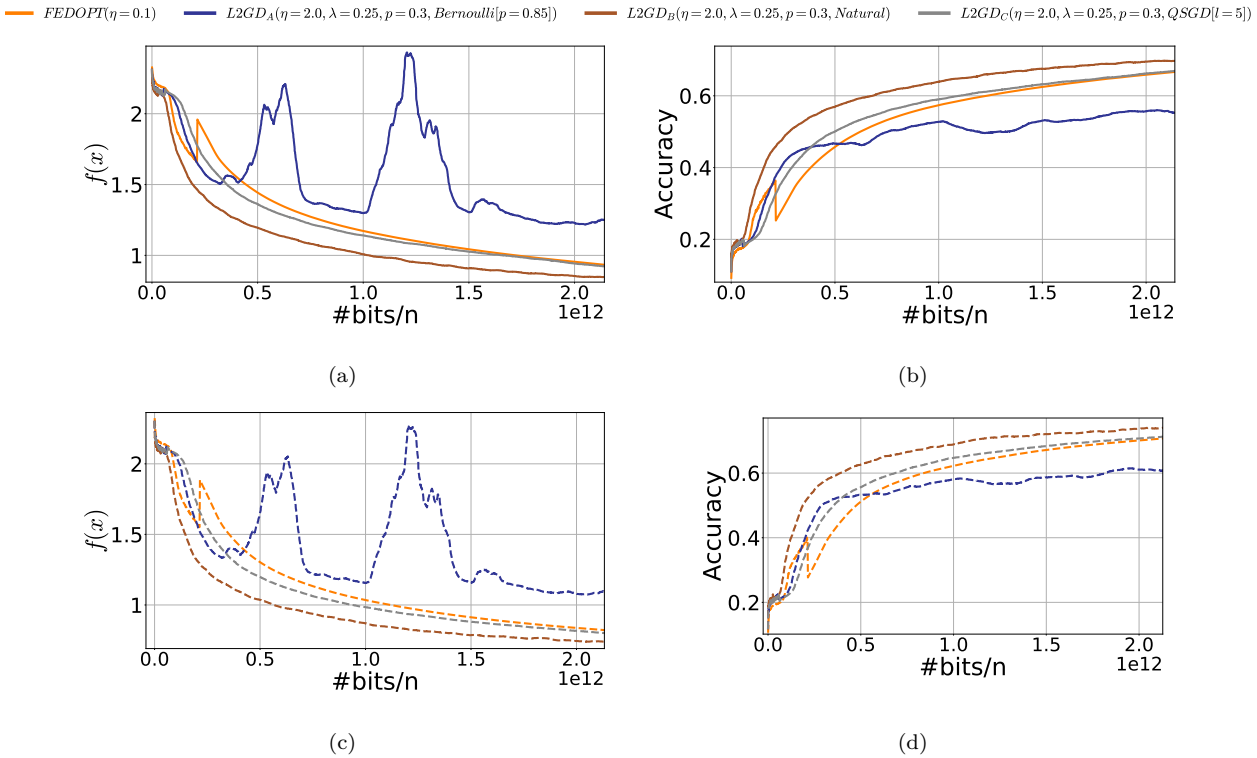

Figure 8: Training `ResNet-18` on `CIFAR-10`, with $n = 10$ workers. Loss and Top-1 accuracy on train (a) - (b) and test data (c) - (d).

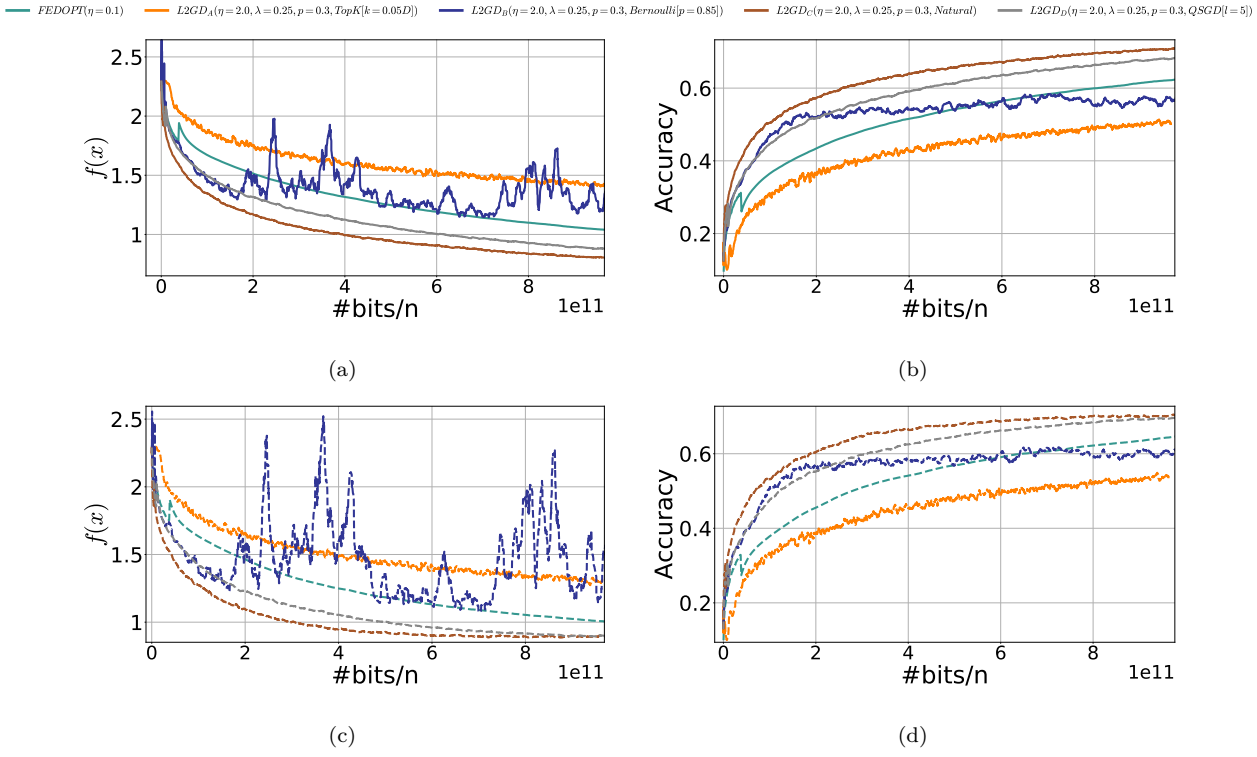

Figure 9: Training `DenseNet-121` on `CIFAR-10`, with $n = 10$ workers. Loss and Top-1 accuracy on train (a) - (b), and test data (c) - (d).

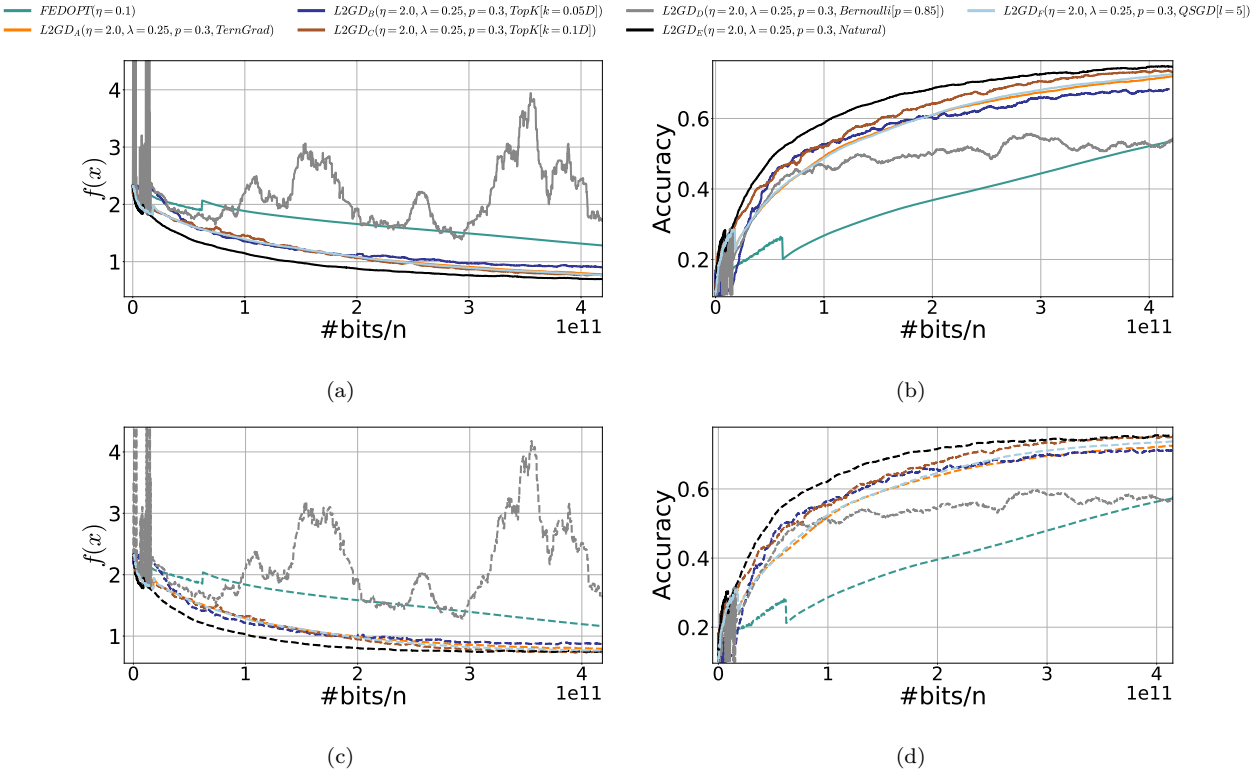

Figure 10: Training `MobileNet` on `CIFAR-10`, with $n = 10$ workers. Loss and Top-1 accuracy on train (a) - (b), and test data (c) - (d).